UPPSALA
UNIVERSITET

Digital Comprehensive Summaries of Uppsala Dissertations from the Faculty of Science and Technology 1304

The Use of Press Archives in the Temporal and Spatial Analysis of Rainfall-Induced Landslides in Tegucigalpa, Honduras, 1980-2005

ELIAS GARCIA-URQUIA

ACTA
UNIVERSITATIS
UPSALIENSIS
UPPSALA
2015

ISSN 1651-6214
ISBN 978-91-554-9375-2
urn:nbn:se:uu:diva-264645

Dissertation presented at Uppsala University to be publicly examined in Polhemssalen, Ångströmlaboratoriet, Lägerhyddsvägen 1, Uppsala, Thursday, 3 December 2015 at 10:15 for the degree of Doctor of Philosophy. The examination will be conducted in English. Faculty examiner: Senior scientist José Cepeda (Norwegian Geotechnical Institute).

Abstract
Garcia-Urquia, E. 2015. The Use of Press Archives in the Temporal and Spatial Analysis of Rainfall-Induced Landslides in Tegucigalpa, Honduras, 1980-2005. *Digital Comprehensive Summaries of Uppsala Dissertations from the Faculty of Science and Technology* 1304. 90 pp. Uppsala: Acta Universitatis Upsaliensis. ISBN 978-91-554-9375-2.

The scarcity of data poses a challenging obstacle for the study of natural disasters, especially in developing countries where the social vulnerability plays as important a role as the physical vulnerability. The work presented in this thesis is oriented towards the demonstration of the usefulness of press archives as a data source for the temporal and spatial analysis of landslides in Tegucigalpa, Honduras for the period between 1980 and 2005. In the last four decades, Tegucigalpa has been characterized by a disorganized urban growth that has significantly contributed to the destabilization of the city's slopes. In the first part of the thesis, a description of the database compilation procedure is provided. The limitations of using data derived from press archives have also been addressed to indicate how these affect the subsequent landslide analyses. In the second part, the temporal richness offered by press archives has allowed the establishment of rainfall thresholds for landslide occurrence. Through the use of the critical rainfall intensity method, the analysis of rainfall thresholds for 7, 15, 30 and 60 antecedent days shows that the number of yielded false alarms increases with the threshold duration. A new method based on the rainfall frequency contour lines was proposed to improve the distinction between days with and without landslides. This method also offers the possibility to identify the landslides that may only occur with a major contribution of anthropogenic disturbances as well as those landslides induced by high-magnitude rainfall events. In the third part, the matrix method has been employed to construct two landslide susceptibility maps: one based on the multi-temporal press-based landslide inventory and a second one based on the landslide inventory derived from an aerial photograph interpretation carried out in 2014. Despite the low spatial accuracy provided by the press archives in locating the landslides, both maps exhibit 69% of consistency in the susceptibility classes and a good agreement in the areas with the highest propensity to landslides. Finally, the integration of these studies with major actions required to improve the process of landslide data collection is proposed to prepare Tegucigalpa for future landslides.

Keywords: press archives, landslide database, urban landslides, critical rainfall intensity, antecedent rainfall, rainfall frequency contour lines, matrix method, landslide susceptibility index, Tegucigalpa, Honduras, Hurricane Mitch

Elias Garcia-Urquia, Applied Mechanics, Byggteknik, 516, Uppsala University, SE-751 20 Uppsala, Sweden.

ISSN 1651-6214
ISBN 978-91-554-9375-2
urn:nbn:se:uu:diva-264645 (http://urn.kb.se/resolve?urn=urn:nbn:se:uu:diva-264645)

Dedicada a Reina, Vilma y Denisse,
gracias por todos estos años de
comprensión, paciencia
y motivación

List of Papers

This thesis is based on the following papers, which are referred to in the text by their Roman numerals.

I Garcia-Urquia, E., Axelsson, K. (2014). The use of press data in the development of a database for rainfall-induced landslides in Tegucigalpa, Honduras, 1980-2005. *Natural Hazards*, 73(2):237–258.

II Garcia-Urquia, E., Axelsson, K. (2015) Rainfall thresholds for the initiation of urban landslides in Tegucigalpa, Honduras: An application of the critical rainfall intensity. *Geografiska Annaler Series A Physical Geography*, 97(1): 61-83.

III Garcia-Urquia, E. (2015) Establishing Rainfall Frequency Contour Lines as thresholds for rainfall-induced landslides in Tegucigalpa, Honduras. *Under revision for Natural Hazards.*

IV Garcia-Urquia, E., Yamagishi, H. (2015) Comparison of landslide susceptibility maps derived from press-based and aerial photograph interpretation inventories for Tegucigalpa, Honduras. *Manuscript*.

All papers are based on the data collected from press archives and stored in the Rainfall-induced Landslide Database for Tegucigalpa, Honduras, 1980-2005 (available online at DiVA). I was responsible for the collection of data from the press archives and I took part in the scrutiny of the newspapers. Also, I performed the evaluation of the landslide events and the compilation of the database. In all papers, I designed the methods and performed the analyses. I also wrote the papers taking into consideration the advice and feedback from the respective co-authors. Reprints were made with permission from the respective publishers.

Contents

Acronyms

Acronyms	Full name
API	Aerial Photograph Interpretation
CRI	Critical Rainfall Intensity
FPR	False Positive Rate
JICA	Japanese International Cooperation Agency
LD	Landslide Day
LSI	Landslide Susceptibility Index
NLD	Non-landslide Day
PB	Press-based
RFCL	Rainfall Frequency Contour Lines
ROC	Receiver Operating Characteristic
TH	Threshold
THS	Threshold Set
TPR	True Positive Rate
USGS	United States Geological Survey

1. Introduction

1.1 Honduras and its vulnerability to natural disasters

A recent study on the worldwide impact of natural disasters has revealed that nine of the ten most affected countries during the period 1994-2013 were developing countries (Kreft, 2014). The occurrence of Hurricane Mitch in October of 1998, considered to be one of the deadliest Atlantic hurricanes in history (Pielke et al., 2003) has been decisive for the ranking of three Central American countries in this list: Honduras has long been in the first place, followed by Nicaragua (Rank 4) and Guatemala (Rank 9) (Kreft, 2014). Unfortunately, natural disasters have a greater impact in developing countries due to their unfavorable geographic location and the economic, social, political and cultural conditions of their residents (Alcántara-Ayala, 2002). While it is true that the Central American region has a rich history of floods, storms, earthquakes, volcanic eruptions and landslides that significantly contributes to the natural vulnerability of the area (Alcántara-Ayala, 2009; Bommer & Rodríguez, 2002; Nadim et al., 2006; Sepúlveda & Petley, 2015), these natural hazards have become disasters due to the lack of a proper risk management to prevent, mitigate and reduce their negative effects on society (Mora, 2009).

The economical and social conditions in Honduras play as important a role in the country's vulnerability to disasters as its exposure to natural hazards. A recent study on the chronic poverty in Latin America shows that Honduras has the second highest percentage of population that has remained poor from 2004 to 2012 and one of the highest percentages of population that were non-poor in 2004 but had fallen into poverty in 2012 (Vakis, 2015) In addition, the population in Honduras also has the lowest levels of positive future expectations, possibly aggravated by the fact that the number of social programs aiming at national poverty reduction has also been one of the lowest in the region (Vakis, 2015). In this context, the chronic poor in Honduras lack enough opportunities to pull themselves out of poverty and are willing to do anything to improve their lifestyle. Consequently, many people living in the rural areas have migrated to the major cities in search for better job opportunities and Tegucigalpa, being the capital city, has had the highest migration rate in the last decades (Angel et al., 2004). Due to the lack of a proper urban plan, Tegucigalpa has not been able to expand appropriately to accommodate the migrants and many end up living in unsuitable areas. Un-

fortunately, these poor people have become the most vulnerable group to disasters induced by natural hazards and have been forced to accept high levels of risk to disasters (Winter & Bromhead, 2012), namely landslides and floods.

1.2 Landslides in Tegucigalpa, Honduras

Tegucigalpa has a long history of landslides that can be traced back to the reactivation of the city's biggest landslide, El Berrinche, as a result of the passage of Hurricane Fifi in 1974 (van Westen et al., 2008). In October of 1998, the city experienced a unique episode of numerous landslides and flooding as a result of Hurricane Mitch. Since then, despite the fact that the written media inform about the occurrence of landslides every year during the rainy season, very few landslides studies have been performed, as shown in Table 1 (see **Paper IV)**. This is very likely due to the reduced number of landslide experts in the country (Yamagishi et al., 2014) coupled with the lack of a scientific unit capable of analyzing and characterizing the landslides and keeping a proper record of the city's landslide activity. As a result, not only are there very few landslide data generated but also, much of the available data contain errors that compromise the reliability of the studies built upon them (Westerberg et al., 2010). As with other developing countries, the lack of data has represented a challenge for various teams studying the occurrence of landslides and other natural disasters. For example, the United States Geological Survey (USGS) conducted extensive fieldwork and aerial photograph interpretation in 2001 and developed an event-based landslide inventory after the occurrence of Hurricane Mitch (Harp et al., 2002). However, due to the lack of a proper geotechnical characterization of Tegucigalpa's geological units, the research team had to adopt the shear strength parameters from similar geological units in California and Washington to establish a deterministic susceptibility map (Harp et al., 2009).

1.3 Aims of the thesis

While the study of anomalous natural events like Hurricane Mitch is essential in order to understand the conditions that contribute to the vulnerability of the city, the study of high-frequency lesser events is equally important. The previous landslide investigations in the study area have been restrained by the limited amount of data and therefore, it is necessary to explore other sources of data that can provide valuable information of the city's past landslide activity. Therefore, the general aim of the thesis is to demonstrate the usefulness of data derived from press archives for the temporal and spatial analyses of rainfall-induced landslides in the urban area of Tegucigalpa,

Honduras between the years 1980 and 2005 (See Figure 1 for a general overview). The experiences provided herein may inspire researchers around the world to undertake similar studies in data-scarce regions with disorganized growth and with frequent disasters. The specific aims of the thesis are:

- Development of the press-based database and assessment of its limitations and possible applications (**Paper I**)
- Analysis of short, medium and long term rainfall thresholds for landslide occurrence based on the triggering rainfall (i.e. the rainfall that prompted the landslide) and the antecedent rainfall (i.e. the rainfall accumulated over a determined number of days prior to the landslide) (**Paper II**)
- Establishment of a graphical method for the definition of rainfall thresholds based on the triggering and the short-term antecedent rainfall (i.e. the rainfall accumulated over a few days prior to landslide occurrence) (**Paper III**)
- Construction of a landslide susceptibility map based on the press-based landslide inventory and comparison with a landslide susceptibility map derived from aerial photograph interpretation in 2014 (**Paper IV**).

Table 1. *Landslide studies in Tegucigalpa, Honduras*

Source	Scale	Outcome
(van Westen et al. 2008)	El Berrinche Hill	Analysis of evolution of the biggest landslide in the city and comparison of landslide inventories for Hurricane Mitch
(JICA, 2002)	Tegucigalpa	Event-based landslide inventory map and modeling of El Reparto and El Berrinche landslides
(Harp et al., 2002; Harp et al., 2009)	Tegucigalpa	Event-based landslide inventory and deterministic landslide susceptibility map
(Pineda, 2004)	Tegucigalpa	Heuristic landslide susceptibility map
(Frigerio & van Westen, 2010)	Tegucigalpa	Establishment of training package for landslide assessment
(Flores Peñalba et al., 2009)	El Berrinche Hill	Probabilistic analysis of failure and establishment of remedial measures for El Berrinche landslide
(UNDP-DIPECHO, 2010, 2012)	Selected neighborhoods	Evaluation of preparedness to future landslides
(Yamagishi et al., 2014)	Tegucigalpa	Landslide inventory based on aerial photograph interpretation (API)

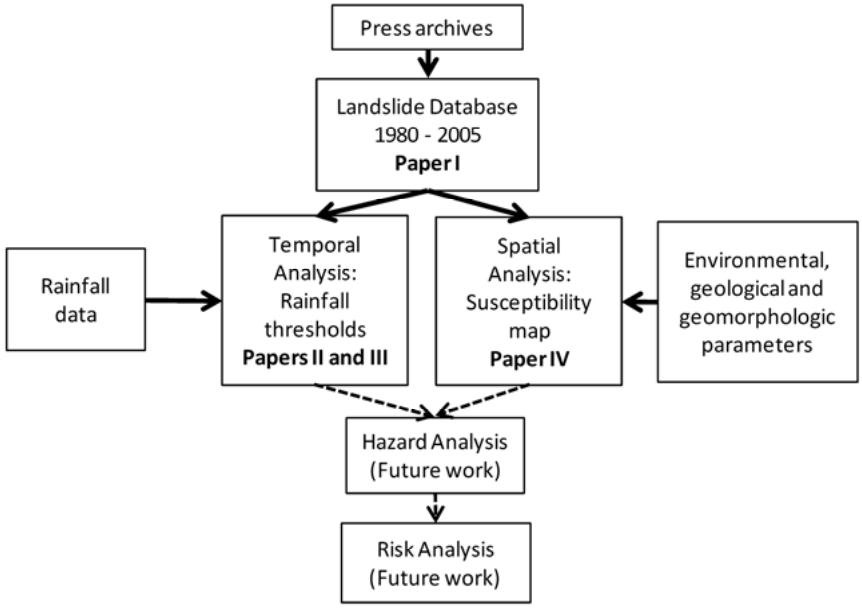

Figure 1. Overview of the landslide studies covered in this thesis

2. Theoretical Background

2.1 Development of historical databases

Researchers worldwide have developed historical landslide databases based upon newspaper and magazine articles, technical reports, post-graduate theses, scientific publications and other useful documents. For example, significant efforts have been directed in recent times to the creation of the DESINVENTAR online database, which contains data pertaining to landslides and other natural disasters mainly for the Latin American region (DESINVENTAR, 2013). **Paper I** provides a brief overview of some of the landslide databases at a regional, national and global scale described in the scientific literature. All of these studies have demonstrated unique aspects of the use of historical documents in landslide investigations.

To improve the assessments at a regional level, Ibsen & Brunsden (1996) have incorporated a moisture balance into the temporal analysis of landslide initiation while Carrara et al. (2003) and Calcaterra et al. (2003) have combined historical data with geomorphologic and geological data to obtain a better understanding of the spatial occurrence of landslides. Combined temporal and spatial analyses have also led to the development of landslide hazard maps (Glade, 2001) and landslide recurrence time maps (Petrucci & Polemio, 2003). Meanwhile, other researchers have considered important to show how the press influences perception of risk (Llasat et al., 2009), how inventories may vary between regions of the same country (Raska et al., 2013) and how the use of monitoring devices has contributed to an enhanced detection of landslides in recent years (Marchi & Tecca, 2006; Tropeano & Turconi, 2004) .

At the national level on the other hand, researchers have been interested in analyzing the damages left by landslides, leading to maps showing the cost of damage (Hilker et al., 2009), an index to compare landslide-induced casualties between countries (Guzzetti, 2000), and the portrayal of the deadliest events (Alcántara-Ayala, 2008; Guzzetti, 2000). In addition, the importance of national databases to society has been exposed by Devoli et al. (2007b) and Foster et al. (2012). Finally, at the global scale, Petley et al. (2005) have analyzed the geographical and temporal occurrence of landslide casualties while Kirschbaum et al. (2010) have evaluated the correlation between landslide occurrence and landslide reports in different regions.

One of the most important topics of discussion concerning these studies is the limitations of the historical documents as sources of data for landslide studies. Because many of the historical documents widely used for the construction of landslide databases have not been developed for scientific purposes, the information pertaining to many landslides is filtered out. Table 2 provides an overview of the most commonly overlooked landslides. It can be seen that the likelihood of a historical landslide to be included in a database depends on: a. its relative importance to society when it occurred (Documentation stage); b. its availability in the historical records through time (Search for Records stage); and c. the easiness with which its associated information can be accurately interpreted (Database Compilation stage). Despite the restrictions that impede the achievement of complete catalogues, all research teams have used the resulting inventories to obtain a better understanding of the occurrence of landslides in the study areas.

2.2 Rainfall thresholds

One of the most common applications of historical database compilations is the establishment of rainfall thresholds for landslide occurrence. Rainfall-induced landslides have two main mechanisms: erosion by surface water runoff and shear failure due to pore-water pressure build-up (Nadim et al., 2009). Therefore, it is necessary to analyze different characteristics of the rainfall events that have induced landslides. Guzzetti et al. (2007) provide a thorough review of different methods that have been applied worldwide. The selection of the method significantly depends on several factors such as landslide failure depth, the rainfall regime, failure mechanism and the physical characteristics of the soil, but most importantly, on the availability of data concerning the triggering agent.

The construction of rainfall thresholds requires the identification of the *triggering rainfall*, which can be defined as the rainfall that directly prompted the landslide. However, the unavailability of data concerning the exact time of landslide occurrence and/or hourly rainfall records may represent a significant obstacle. Figure 2 shows that ideally, the rainfall accumulated during the first 6 hours of the rainfall event on "day x" would constitute the triggering rainfall for a landslide occurring in position C. Likewise, the total amount of rainfall accumulated for this event would constitute the triggering rainfall for a landslide in position E. Yet, these landslides are usually regarded as occurring in position D (i.e. at the end of the rainfall event) if there is lack of knowledge on the time of occurrence of the landslide or the distribution of rainfall during the event. In the case of a landslide occurring in position B, the triggering rainfall is that of "day x-1", even though the landslide actually occurred on "day x". The landslide is then regarded as occur-

Table 2. *Commonly overlooked landslides in historical documents*

Stage	Description of Landslide	Sources
Documentation: At the time of occurrence, is the landslide worth documenting?	• Landslides that have caused no damage to humans or nearby infrastructure	b, d, g, k, l, o
	• Landslides that have occurred in unpopulated areas, for which no witnesses were present	a, b, c, f, h, i, j, m, n, p
	• Landslides that have occurred during unstable periods (e.g. political conflicts or wars) that overshadow their occurrence	c, h, n
	• Landslides that have occurred simultaneously with other natural hazards (other landslides, floods or storms) that have been more attractive to document	a, c, f, h, j, m
Search for Records: Is the landslide easily detected in the available historical sources in time?	• Minor landslides that were not documented as these occurred in the far past when the documenting threshold remained high	e, f, h, l, m
	• Landslides that have been documented in sources not commonly investigated (e.g. religious publications or local archives)	a, l
	• Landslides that have occurred in regions with very few historical archives available	g, p, q
Database Compilation: Can the information provided in the sources be accurately interpreted?	• Landslides for which the term has been employed incorrectly (often reported as floods) or not mentioned at all in the sources	a, f, g, l, m
	• Landslides having qualitative adjectives describing its characteristics (e.g. big, many, intense)*	c, f , h, i, o
	• Landslides for which contradictory datasets exist and whose validation is not possible*	c, f, h

Sources: a = (Calcaterra et al., 2003), b = (Carrara et al., 2003), c = (Devoli et al., 2007a), d = (Domínguez Cuesta et al., 1999), e = (Glade, 2001), f = (Guzzetti, 2000), g = (Hilker et al., 2009), h = (Ibsen & Brunsden, 1996), i = (Kalantzi et al., 2010), j = (Kirschbaum et al., 2010), k = (Llasat et al., 2009), l = (Marchi & Tecca, 2006), m = (Petley et al., 2005), n = (Petrucci & Polemio, 2003), o = (Petrucci et al., 2009), p = (Raska et al., 2013), q = (Tropeano & Turconi, 2004).

* = these landslides are, most of the time, included in the databases but their associated information possesses a high degree of uncertainty.

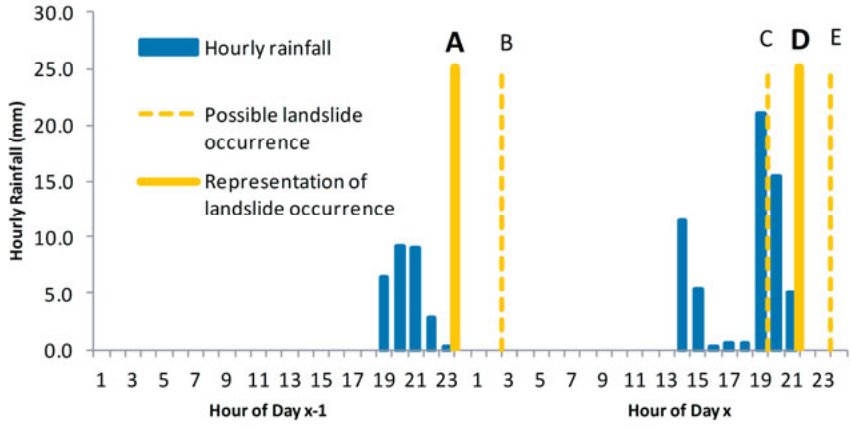

Figure 2. Assumptions made for the definition of a landslide's triggering rainfall when data concerning the exact time of occurrence and/or hourly rainfall records are unavailable. Under such circumstances, landslides occurring in position C and position E are regarded as occurring in position D (i.e. at the end of the rainfall event on "day x") and the triggering rainfall is that of "day x". Meanwhile, a landslide occurring in position B would be treated as occurring in position A and therefore, the triggering rainfall is that of "day x-1".

ring in position A and thus, the "day x-1" may be considered the Landslide Day (LD).

Many research teams have acknowledged the importance of analyzing the contribution of rainfall events in the days prior to the day of landslide occurrence (hereafter known as *antecedent rainfall*). Because landslides are a result of the interaction of many factors that vary significantly across the world (e.g. rainfall intensities and the soil's hydraulic properties), there is no consensus on the appropriate amount of antecedent days to consider. It is therefore necessary to analyze different antecedent durations for each LD and different threshold durations to establish a suitable threshold line that offers a good predictive performance. For example, Figure 3a shows the triggering rainfall (i.e. the rainfall on Day 0 of the antecedent scale, shown in yellow) and the antecedent rainfall of a LD considered for the construction of the 15-day threshold line in red. In this scenario, the antecedent rainfall of 8 days may have been crucial for the occurrence of the landslide, since this rainfall amount exceeds the rainfall demands of the threshold (i.e the green dot on the 8^{th} antecedent day lies above the red line). Alternatively, the antecedent rainfall of 4 days also exceeds the rainfall demands of the threshold line. However, when the *threshold duration* is reduced to 7 days (see Figure 3b), the rainfall amounts occurring on the 8^{th} and 9^{th} antecedent day for the same LD are disregarded. In such case, the only critical event is the rainfall accumulated over an *antecedent duration* of 4 days.

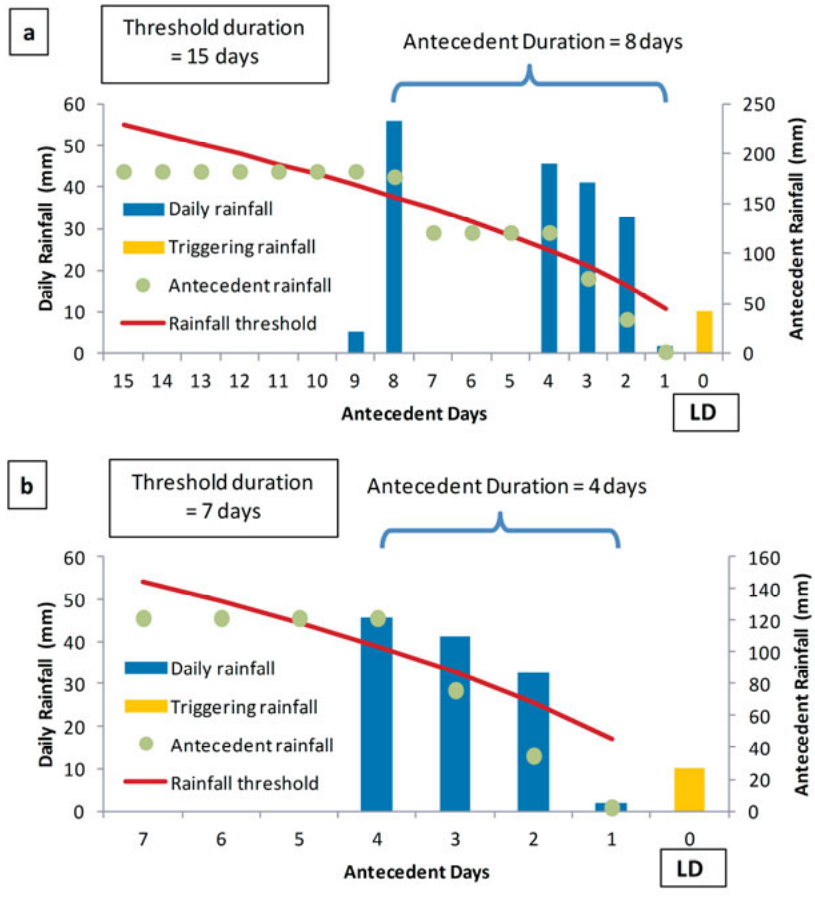

Figure 3. Relationship between triggering rainfall, antecedent rainfall, antecedent duration and threshold duration. The yellow bar shows the triggering rainfall (i.e. the rainfall occurring on Day 0 of the antecedent scale) for a LD. The blue bars show the daily rainfall for several days previous to the day of landslide occurrence. a) When the threshold duration is 15 days, the antecedent rainfall corresponding to 8 days may have contributed to landslide occurrence, since the green dot on the 8th antecedent day lies above the threshold line in red. b) When the threshold duration is reduced to 7 days, the critical event is the antecedent rainfall of 4 days.

Paper II addresses numerous case studies that have recognized the importance of antecedent rainfall as the controlling agent of the soil moisture in slopes (Jemec & Komac, 2012; Khan et al., 2012; Terlien, 1998). One of the most common approaches is to establish the frequency of high-magnitude rainfall events responsible for landslide occurrence (Floris & Bozzano, 2008; Frattini et al., 2009; Petrucci & Pasqua, 2009; Polemio & Sdao, 1999). Other researchers have tried to determine the antecedent rainfall duration that allows the best discrimination between landslide and non-landslide events (Bui et al., 2013; Dahal & Hasegawa, 2008; Terlien, 1998). Sengupta et al.

(2010) acknowledge the contribution of both antecedent and triggering rainfall by showing that landslides in Sikkim, India, do not occur on days of extreme rainfall and have established a rainfall threshold based on a 15-day cumulative rainfall of 250 mm. Ibsen & Casagli (2004) show that in the Porretta-Vergato region of Italy, antecedent rainfall as far back as 6 months prepares the terrain for failure, while an intense storm is needed to trigger landslides. Mathew et al. (2013) have coupled an Intensity-Duration threshold with a probabilistic assessment of antecedent rainfall to evaluate landslide occurrence in the Indian Himalayas. Similarly, Gabet et al. (2004) have concluded that while regolith thickness has influence over the seasonal rainfall accumulation in the Nepalese Himalayas, slope angle controls the daily rainfall required to initiate landslides.

Paper III stresses the importance of daily vs. antecedent rainfall plots to assess landslide occurrence (Chleborad et al., 2006; Dahal & Hasegawa, 2008; Kanungo & Sharma, 2014; Zezêre et al., 2015). While some studies have relied on them for the evaluation of the temporal occurrence of landslides (Bai et al., 2014; Jaiswal & van Westen, 2009), others have integrated them into the temporal and spatial analysis of landslide occurrence for the elaboration of hazard maps (Bui et al. 2013; Althuwaynee et al., 2014) and risk maps (Erener & Duzgun, 2013).

One of the key aspects of threshold construction is the predictive performance in distinguishing between days with and without landslides. The trustworthiness of a rainfall threshold not only depends on its capability of underlying as many landslide-triggering rainfall events as possible but also on differentiating these events from those that have not produced landslides (Zezêre et al., 2015). Therefore, a careful evaluation of the predictive performance of any threshold line should always be presented, especially in the case where antecedent rainfall plays a significant role in landslide occurrence. The ideal antecedent duration for the study area is usually selected based on the plot whose threshold line yields the best discriminative power. For such purpose, diagonal dividers that assign equal weights of importance to the daily and antecedent rainfall (Dahal & Hasegawa 2008; Kanungo & Sharma, 2014) and envelope lines that connect the lowest points in the plots (Althuwaynee et al., 2014; Bui et al., 2013; Chleborad et al., 2006; Jaiswal & van Westen, 2009) are frequently used. However, these techniques may not produce reliable thresholds for the study of urban landslides, since the disturbances of mankind significantly alter the relationship between rainfall and slope failures.

2.3 Landslide susceptibility mapping

The construction of landslide susceptibility maps requires a reliable landslide inventory and spatial data related to landslide occurrence. Landslide inven-

tories are commonly generated after the occurrence of an anomalous event capable of triggering a widespread initiation of landslides. In some study areas, efforts have been made to compile historical inventories involving several triggering events. Knowledge of the geomorphologic, geological and environmental factors that have contributed to landslide occurrence is also essential for the identification of places where landslides are likely to occur. Slope angle, elevation, aspect, geology, distance to faults and distance to roads are among the most commonly studied variables. The scale and the availability of data related to these preparatory factors usually dictates the method to be employed for the spatial assessment (van Westen et al., 2008).

Table 3 (from **Paper IV)** provides an overview of several methods that have been proposed in the scientific literature to produce landslide susceptibility maps (Pardeshi et al., 2013). All of these methods rely on bivariate or multivariate statistical or probabilistic analyses to relate the preparatory factors to the occurrence of past landslides. Logistic regression is a multivariate statistical approach employed to find a function that relates the presence or absence of landslides to a set of independent parameters (Ayalew & Yamagishi, 2005). Artifical neural networks (ANNs) consist of a collection of neurons that evaluate non-linear functions of their inputs. Through the establishment of an algorithm, the weights assigned to the input are adjusted until a minimal error between the target and output values is achieved. The trained network is then able to distinguish between landslide-prone and stable areas (Pradhan & Lee, 2010). The frequency ratio expresses the ratio of the probability of a landslide occurrence to the probability of no landslide occurrence for a given variable. When the ratio is greater than 1, the relationship between the variable's range and the landslide occurrence is strong (Lee & Sambath, 2006) The matrix method requires the determination of all possible combinations of three variables and for each combination, the ratio of landslide cells to the total amount of cells is established (Irigaray et al., 2007). In the Analytical Hierarchy Process (AHP), the landslide-related factors are subjectively assigned values from 1 to 9 based on the relative importance to landslide occurrence. Weights are then calculated for each factor in a pairwise comparison matrix (Ayalew et al., 2005). In the weighted linear combination method, primary level weights are assigned to each class of a particular parameter, while secondary level weights are assigned to the parameters through a pairwise comparion matrix. All the weights are then combined into a single map (Ayalew et al., 2004). For the weights of evidence method (WoE), the weights for each landslide factor are calculated based on the presence or absence of landslides using the Bayesian probability model (Dahal et al., 2008).

Table 3. *Common methods employed in landslide susceptibility studies*

Authors	Study Area	Susceptibility Methods						
		LRe	ANN	FRa	Mat	AHP	WLC	WoE
(Ayalew & Yamagishi, 2005)	Kakuda-Yahiko Mountains, Central Japan	X						
(Bui et al., 2013)	Hoa Binh province, Vietnam	X						
(Chen & Wang, 2007)	Mackenzie Valley, Canada	X						
(Dai et al., 2004)	Lantau Island, Hong Kong	X						
(Duman et al., 2006)	Cekmec Area, Istanbul, Turkey	X						
(Lee & Pradhan, 2007)	Selangor, Malaysia	X		X				
(Lee & Sambath, 2006)	Damrei Romel area, Cambodia	X		X				
(Lepore et al., 2012)	Puerto Rico	X		X				
(Pradhan & Lee, 2010)	Penang Island, Malaysia	X	X	X				
(Süzen & Doyuran, 2004)	Asarsuyu catchment, NW Turkey	X						
(Yalcin et al., 2011)	Trabzon, NE Turkey	X		X		X		
(de Souza & Ebecken, 2012)	Rio de Janeiro City		X					
(Melchiorre et al., 2008)	Brembilla Municipality, Southern Alps, Italy		X					
(Akgun et al., 2008)	Findikli district, Rize, Turkey			X			X	
(Costanzo, et al., 2012)	Beiro River basin, Spain				X			
(Cross, 1998)	Peak District, Derbyshire, United Kingdom				X			
(De Graff et al., 2012)	Dominica and Jamaica				X			
(Fernández et al., 2003)	Contraviesa área, Granada, Spain				X			
(Irigaray et al., 2007)	Betic Cordillera, southern Spain				X			
(Jiménez-Perálvarez et al., 2009, 2011)	Sierra Nevada, Granada, Spain				X			
(Ayalew et al., 2005)	Sado Island, Japan					X		
(Ayalew et al., 2004)	Tsugawa área of Agano River, Niigata Prefecture, Japan						X	
(Dahal et al., 2008)	Lesser Himalaya of Nepal							X
(Regmi et al., 2010)	Western Colorado, USA							X

LRe = Logistic Regression, ANN = Artificial Neural Network, FRa = Frequency Ratio, Mat = Matrix Method, AHP = Analytical Hierarchy Process, WLC = Weighted Linear Combination, WoE = Weights of Evidence

3. Study Area

Tegucigalpa is located in a mountainous basin in the southern central region of Honduras (see Figure 4 for location). The elevation ranges from 900 to 1400 meters above sea level. In 2001 (close to the end of the study period), Tegucigalpa occupied an area of nearly 100 km^2 and was home to 850,000 inhabitants (JICA, 2002). The temperature varies between 19 and 23 °C all year round. The city experiences two seasons: the rainy season, which extends from May to October and the dry season, which covers the November-April period. However, there are some sporadic rainfall events in April and November. During the rainy season, 870 mm of rainfall are recorded on average, September being the wettest month. The city has a very complex geological setting (JICA, 2002) and due to the warm year-round temperatures and the intense rainfall events, many rocks suffer moderate weathering that makes them prone to landslides. In addition, the Choluteca River, its tributaries and approximately 18 creeks fractionate the city and pose serious threats to the residents during the rainy season due to the erosive forces on the slopes.

Figure 4. Location of Tegucigalpa, Honduras.

In the last 40 years, Tegucigalpa has suffered from a disorganized urban growth. The insufficient housing and the relatively high costs of living in safe areas where basic needs such as water and electricity are satisfied, drives rural newcomers and local residents with limited resources to live illegally in places not suitable for construction (Angel et al., 2004). In many cases, the extreme poverty of these families forces them to build their own homes, utilizing inappropriate building techniques and low-quality materials (ECLAC, 1999). Despite the evident dangers of living in these risky areas, the lack of job opportunities in other smaller settlements nearby forces many residents to stay in the periphery of the city and cope with the risks of landslides and floods every year (Pearce-Oroz, 2005). Even though laws prohibiting the establishment of settlements in risky areas do exist, the local governments have failed in enforcing control of these policies (Fay et al., 2003). A clear example of this weak control was left in evidence in October 1998 during the passage of Hurricane Mitch, which triggered numerous landslides and extensive flood throughout the city (Harp et al., 2002). The most damaging landslide episode occurred in El Berrinche, a densely-populated hill that collapsed and dammed the Choluteca River for several days. The losses caused by this landslide would have been significantly reduced if the territorial policies prohibiting development in this neighborhood and which were elaborated in the 1970s would have been properly enforced (Cascini et al., 2005).

In recent years, it has been estimated that nearly 40% of the population of Tegucigalpa lives in illegal settlements and at least six new illegal settlements are established every year (El Heraldo, 2013). In 2014, experts from the Japanese International Cooperation Agency (JICA) and the Japanese Society for the Promotion of Science (JSPS) presented a landslide inventory map based on aerial photograph interpretation to the local authorities (Yamagishi et al., 2014). This map revealed that approximately 500,000 inhabitants living in 176 neighborhoods are at risk of landslides (El Heraldo, 2014). Figure 5 shows some of the landslide-prone neighborhoods in the past years.

Figure 5. a. Location of landslide-prone neighborhoods in Tegucigalpa. b. A household was affected by a landslide in the Guillen neighborhood. c. In the Izaguirre neighborhood, a total of 20 houses suffered damages due to a landslide episode in 2013. d. The Los Pinos neighborhood is constantly exposed to landslides in recent years due to the unfavorable physical conditions and the lack of a proper urban plan. e. The social vulnerability of the residents of the Villanueva neighborhood has forced them to improvise retaining walls built from scrap in an attempt to reduce the damages produced by landslides. f. The residents of the José Angel Ulloa neighborhood are in danger due to the continuous slope failures that threaten to destroy their fragile households. Photos b - f were published by El Heraldo newspaper on the 29 August 2012, 19 September 2013, 23 October 2014, 23 October 2014, and 30 June 2015, respectively.

4. Methods

4.1 Database compilation

Paper I describes the procedure carried out to develop the press-based landslide database that has served as basis for all papers. The two newspapers with main coverage over Tegucigalpa were revised: La Tribuna, founded in 1976 and El Heraldo, founded in 1979. The study was conducted on the physical copies between 1980 and 2005 found in two newspaper libraries in Tegucigalpa. The compilation of the database initiated with the selection of those newspaper articles describing the occurrence of rainfall-induced landslides (See Figure 6 for examples). Those landslides primarily triggered by humans (e.g. due to the use of dynamite to extract rocks from pits or due to the collapse of excavation pits without proper lateral protection in construction sites) were disregarded. Particular focus was given to the following items:

- Place of occurrence: this is the most essential piece of information required for the creation of a landslide entry in the database. Cases in which landslides were said to have occurred but no place was specified were disregarded. Usually, the name of the neighborhood or slum was usually provided and sometimes, the names of well-known buildings or streets (e.g. main road of neighborhood "x" or the school "y" of slum "z") were given as references. In the case of landslides affecting roads, the name of the road was provided but their precise locations were lacking most of the time.
- Date of occurrence: the month and year were usually easily acknowledged, and many times, the exact date was given. When the day of the week was mentioned, the date of occurrence was also considered reliable. However, a certain degree of uncertainty was present when references such as "yesterday" or "two days ago" were specified, as in some cases, the authors of the articles seem to have made such relative temporal references based on the day the article was drafted (i.e. the day before being released to the public) and not the day in which the article was actually read. Seldom, the time of the day was provided (e.g. early morning, afternoon, evening, midnight) and in very few cases, the precise time of occurrence was specified.
- Damages: a vital component of the database is the consequences left behind by the landslide events. The information that can be extracted

Figure 6. Examples of newspaper articles of interest. a. Landslide in Los Pinos in June 2005. b. Landslide in Colonia Soto in August 1988. c. Landslide in El Guanacaste in October 1980. d. Landslide in El Reparto in November 1982. All articles shown were taken from El Heraldo newspaper.

from the newspaper articles includes the number of casualties, the number of injured, the number of homeless (expressed in terms of individuals and/or families), and the physical damages to homes, buildings, roads and other important infrastructure. When multiple landslide events or in combination with a flood occurred simultaneously due to a single rainfall, sometimes it was not possible to determine the damages associated with each of the landslide events, since the overall damages produced by the rainfall were provided. In very few cases, an economical evaluation of the damages has been presented in the articles.

- Causes: in the cases in which moderate to severe damage was produced by the landslides, the articles specified a "possible cause". It is very likely that the cause was obtained from interviews with the affected people or emergency crew members, who may lack the sufficient knowledge to assess the mechanism of failure. Often, the interviewed people claim that recent deficient constructions (e.g. a retaining wall) or public facilities in bad state (e.g. leakage of water pipes) in combination with rainfall have been the causes of landslide events. Only in a few cases have these versions been confirmed or rejected by technical studies. Despite the lack of scientific support, such popular claims have been incorporated as the causes of the landslides in the database.

- Type of movement: unfortunately, this piece of information has been provided rarely and with very low reliability. For a few exceptional cases (e.g. the massive landslide that occurred in El Reparto neighborhood in 1982, and the two major landslides activated during Hurricane Mitch in 1998, El Berrinche and El Reparto), the newspaper articles have summarized the results from professional studies, including the type of movement, following the classification established by Cruden & Varnes, (1996). In all other cases, the reporters have attempted to give accurate descriptions of the movement and materials involved in the displacement, based on interviews with the affected people. These descriptions have also been included in the database as a mere reference.

Paper I also provides some of the limitations encountered during the database compilation and how these can affect the reliability of the database. For example, the ambiguity of the word derrumbe, which is usually translated as "collapse" in English, may have been used by reporters to describe some events that were not landslides. In addition, the style of reporters has been evolving in time and has affected the quantity and quality of the landslide information provided. On the other hand, the occurrence of a landslide followed by slope movements induced by the imminent instability over several days may introduce errors into the construction of the rainfall thresholds discussed in **Papers II and III**. Finally, the unclear spatial references have impeded the achievement of a complete landslide inventory and this affects the reliability of the landslide susceptibility map presented in **Paper IV**.

4.2 Temporal analysis

The temporal analysis of landslide occurrence requires selecting those landslides for which the triggering and antecedent rainfall can be reconstructed based on the rainfall records of the Toncontin Meteorological Station, located to the south of the city. This rainfall station possesses the longest and most reliable rainfall record and is, therefore, considered to be representative for the whole city (JICA, 2002). Two different methods were used: the critical rainfall intensity (**Paper II**) and the rainfall frequency contour lines (**Paper III**). For both analyses, the procedure to reconstruct the antecedent rainfall was the same and is explained in more detail in **Paper II**. While in **Paper II**, the reconstruction of antecedent rainfall involved 19 antecedent durations covering the range between 1 to 60 days, the antecedent range analyzed in **Paper III** is limited to the first 4 days prior to landslide occurrence. This is due to the fact that **Paper II** revealed that out of the four threshold durations analyzed, the shortest duration (i.e. 7-day threshold duration) yielded the best predictive results. In **Paper III**, a new method was proposed to improve the discrimination between Landslide Days (LDs) and Non-

landslide Days (NLDs) by focusing the analysis on the 4 antecedent days prior to landslide occurrence.

4.2.1. Critical Rainfall Intensity

The concept of the critical rainfall intensity (CRI) has been successfully applied in the past by Khan et al. (2012) and Marques et al. (2008) to analyze the contribution of antecedent rainfall to landslide occurrence. It is based on the assumption that intense rainfall events that rarely occur in the studied environment significantly contribute to landslide occurrence. The method involves the determination of the return period using the Gumbel Extreme Value distribution for different cumulative rainfall amounts. The 19 antecedent durations were: 1, 2, 3, 4, 5, 7, 9, 12, 15, 18, 22, 26, 30, 35, 40, 45, 50, 55 and 60 days. **Paper II** also analyzes four threshold durations (i.e. 7, 15, 30 and 60 days) to determine how the predictive performance of the thresholds is affected by the threshold duration.

For each threshold duration, only the rainfall amounts with antecedent durations less than or equal to the threshold duration are considered. For each LD, the return period T (in years) for each of these antecedent rainfall amounts is given by

$$T = \frac{1}{1-e^{-e^{-a(R-x_0)}}}, \quad (1)$$

where $a = \frac{\pi}{\sigma\sqrt{6}}$; σ is the standard deviation of the Gumbel distribution; R is the rainfall amount for which the return period is being determined; $x_o = \mu - \frac{c}{a}$; μ is the mean of the Gumbel distribution and c is the Euler's constant and is equal to 0.577.

For each LD, the antecedent rainfall amount yielding the highest return period was divided by its corresponding antecedent duration to determine the Critical Rainfall Intensity (I).

For a given threshold duration, all LDs are represented by points plotted in a log-log scale (antecedent duration on the x axis, I on the y axis). All thresholds have the form

$$I = aD^b, \quad (2)$$

where I is the Critical Rainfall Intensity (mm/day), D is the corresponding antecedent duration (days), a represents the y intercept of the plot in the log-log scale, and b denotes the slope of the threshold line.

A total of 16 threshold lines were prepared: for each of the 4 threshold durations considered, 4 different levels were analyzed (i.e. the Baseline and the lines underlying 15%, 50%, 85% of all LDs). For each line, a confusion

matrix (see Table 4) was elaborated to determine the number of well-predicted LDs (True Positive), false alarms (False Positive), missed alarms (False Negatives) and well-predicted NLDs (True Negatives). The determination of the True Positive Rate (TPR) and False Positive Rate (FPR), defined as

$$TPR = \frac{TP}{TP+FN} = \frac{Well-Predicted\ LD}{LD} \quad (3)$$

and

$$FPR = \frac{FP}{FP+TN} = \frac{False\ Alarms}{NLD} \quad , \quad (4)$$

respectively, enables the calculation of the Distance to Perfect Classification parameter

$$r = \sqrt{FPR^2 + (1 - TPR)^2} \quad (5)$$

in the Receiver Operating Characteristic (ROC) space, as shown in Figure 7. The r parameter, proposed by Cepeda et al. (2010), is a measure of how poorly a threshold performs in discriminating between LDs and NLDs; the larger the r parameter, the farther away it is from the point of perfect classification in the ROC space.

Table 4. *Confusion Matrix*

Rainfall Threshold Exceedance?	Landslide Occurrence?	
	Yes	No
Yes	True Positive (TP)	False Positive (FP)
No	False Negative (FN)	True Negative (TN)
Σ	LD	NLD

True Positive = well-predicted LD, True Negative = well-predicted NLD, False Positive = false alarms, False Negative = missed alarm

In **Paper II**, the original Critical Rainfall Intensity method was modified to integrate the triggering rainfall into the analysis. Because landslides may occur as a result of a high-magnitude rainfall with little or no contribution from antecedent rainfall, it is reasonable to say that the critical rainfall intensity for those landslides corresponds to the triggering rainfall. In other words, the triggering rainfall for these LDs yields a higher return period than any of the antecedent rainfall amounts. The triggering rainfall can be interpreted as the rainfall occurring on Day 0 of the antecedent scale. For these LDs, the CRI would then be equal to the triggering rainfall amount divided by 1 day (i.e. Day 0), expressed in mm/day. This enables these LDs to be plotted in the line x = 0 of the intensity vs. duration plot shown in Figure 8a.

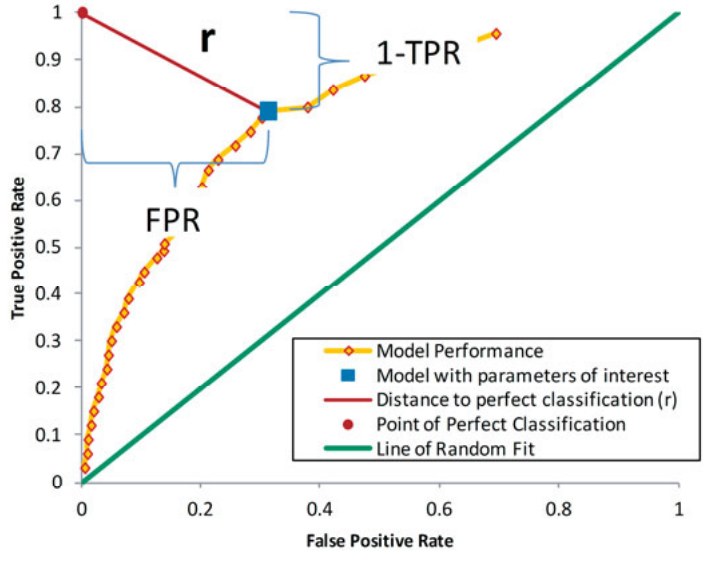

Figure 7. The ROC space where the performance of each threshold is determined. The curve displays the performance of a threshold model: each orange diamond graphically represents a specific set of parameters used to run the model. The x-axis and y-axis represent the proportion of false alarms to NLDs and the proportion of well-predicted LD to LDs respectively, yielded by the model. The point of perfect classification, with coordinates (0,1), represents an ideal model yielding no false alarms and successfully predicting all LD. To indicate how well the model performs in discriminating between LD and NLD with a specific set of parameters, the value of r is determined by measuring the distance between the point representing the set of parameters on the curve (shown as a blue square) and the point of perfect classification. The green line shown represents the Line of Random Fit, and any threshold performance positioned below this line is considered "worse than random".

However, due to the asymptotic behavior of the red power law threshold lines when x = 0, it is not possible to establish a minimum rainfall amount for threshold exceedance. Furthermore, it is not even possible to plot these LDs if the graph has a logarithmic scale. To be able to integrate these LDs into the threshold evaluation, the power law threshold lines may be truncated at a value close to x = 0. In Figure 8b, the threshold lines are truncated at x = 0.1 and then horizontally extended to intersect the y-axis. In this way, the LDs may either be plotted on the line x = 0 or x = 0.1 (see Figure 8c) and the threshold evaluation for rainfall exceedance is not altered. Cutoff values other than x = 0.1 may be chosen, but the closer these lie to 0, the higher the rainfall amounts for threshold exceedance are and the less likely it is to find a daily rainfall value that fulfills the demands of the threshold. Finally, when the intensity vs. duration graph is plotted in logarithmic scale, the threshold lines are simply extended into the new cycle (i.e. 0.1 to 1) and the

LDs are conveniently plotted in the line x = 0.1 (as shown in Figure 8d) to represent the Day 0 of the antecedent scale.

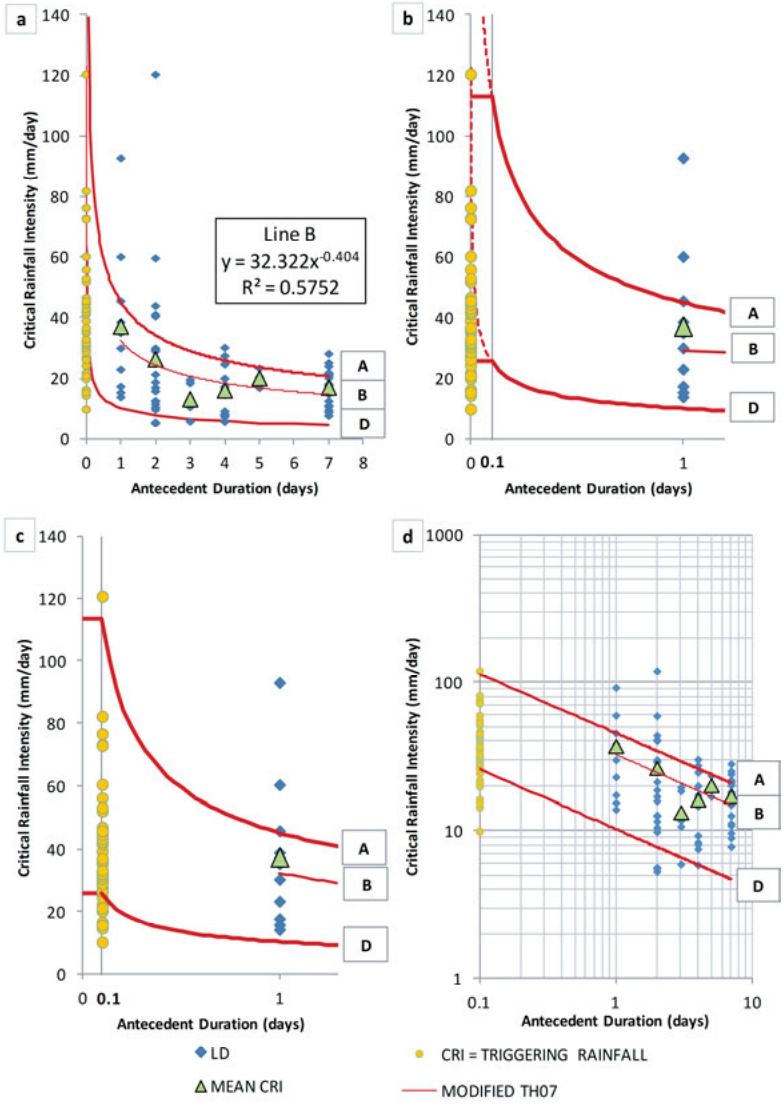

Figure 8. a. Integration of the LDs whose critical rainfall is the triggering rainfall (shown as orange dots) into the line x = 0 of the antecedent scale. b. Truncation of the power law threshold lines (shown in red) at x = 0.1. In the range between 0 and 0.1, the threshold lines assume a horizontal position according to the value at x = 0.1. c. Due to the truncation and horizontal extension of the threshold lines, the orange dots initially lying on the line x = 0 can be shifted to the line x = 0.1 without altering the threshold evaluation for rainfall exceedance. d) In the log-log scale, the threshold lines are extended to the 0.1 – 1 cycle and the orange dots are conveniently placed on the line x = 0.1.

A final adjustment to reduce the number of false alarms was performed by defining a critical region in each triggering vs. antecedent rainfall plot where a combination of triggering and antecedent rainfall is necessary for landslide occurrence. For this purpose, it was necessary to construct triggering vs. antecedent rainfall plots, based on the rainfall values provided by the threshold. For all plots, the triggering rainfall corresponds to that critical value in which no antecedent rainfall is needed for landslide occurrence; this value occurs when D takes the value of 0.1 (see Figure 9a). It was then established that the critical region would cover a range along the antecedent rainfall axis equal to a percentage of the antecedent rainfall amount dictated by the threshold (i.e. AR1 in Figure 9b). For each range, a confusion matrix was produced to determine the number of false alarms and well-predicted LDs (see Figure 9c). An ideal percentage for the critical region has been suggested by analyzing the variation of the ratio of false alarms to well-predicted LDs, with respect to an increasing range of the critical region (Figure 9d). This final adjustment allowed a significant improvement in the predictive performance of the threshold.

4.2.2 Rainfall Frequency Contour Lines

Paper III arose from the need to improve the predictive performance of the threshold proposed in **Paper II**. It introduces a graphical approach for the establishment of rainfall thresholds in the daily vs. antecedent rainfall plots based on the frequency of occurrence of the rainfall events. Based on **Paper II**'s conclusion that the predictive performance of the thresholds is reduced with increasing threshold duration, this method analyzed a period of only 4 antecedent days. For the analysis of each of the four daily vs. antecedent rainfall plots, the following assumptions were considered:

- A day in the study period can be seen as a rainfall pair having a value of daily rainfall and a value of antecedent rainfall. It can be graphically represented as a point in the daily vs. antecedent rainfall plot.
- Two or more rainfall pairs that lie close to each other in any plot represent rainfall combinations with similar magnitudes. To determine the frequency with which these events with similar magnitude have taken place, circular buffers are drawn around all rainfall pairs and a count of points within the buffer is carried out. The point density of each pair is then calculated by dividing the number of points by the area of the buffer. A higher point density means that the event has occurred with a higher frequency.
- The farther the rainfall pairs lie from the origin, the higher the magnitude of the daily and/or antecedent rainfall and the less frequent these rainfall combinations have been. Therefore, the point density of any rainfall combination gradually decreases as it moves away from the origin.

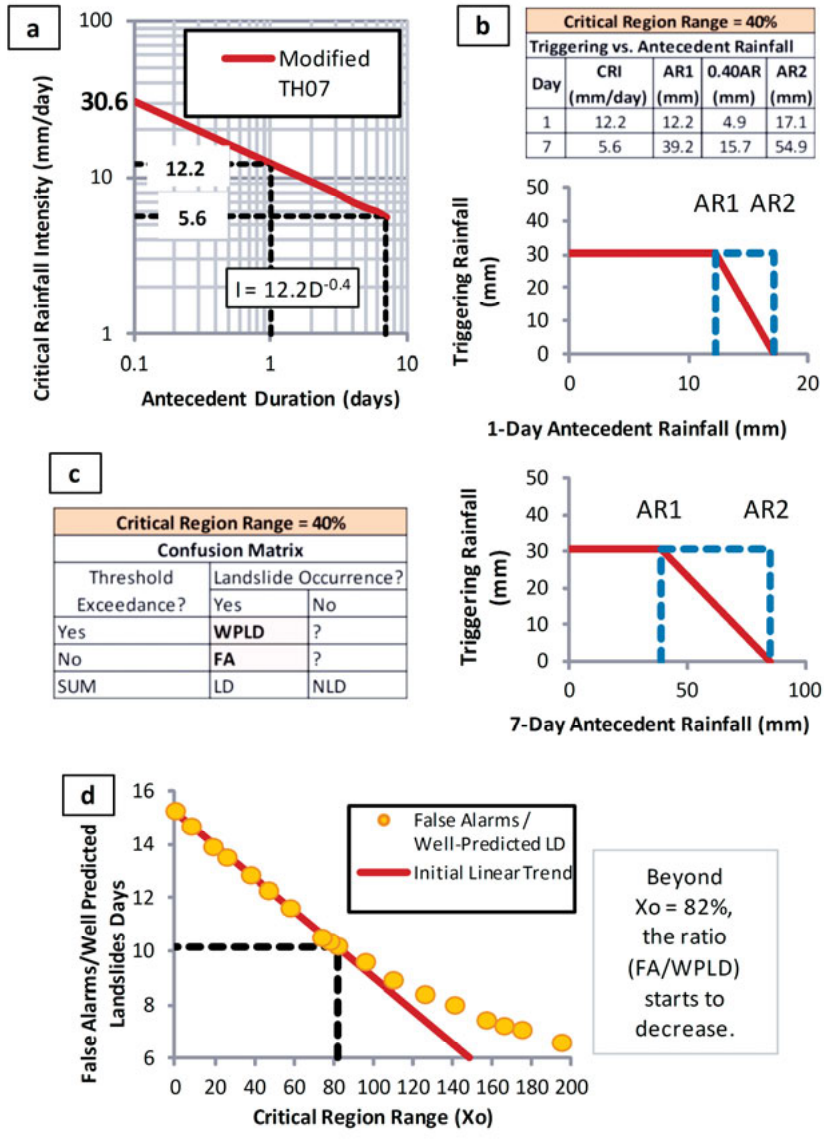

Figure 9. Description of the procedure to define an ideal critical region range (X_0). a. The modified threshold was evaluated to determine the critical triggering rainfall (i.e. when D takes the value of 0.1). In addition, the CRI for all antecedent durations was determined (the example shows the cases of 1 and 7 antecedent days). b. The antecedent rainfall (AR1) was calculated for all antecedent durations. A critical region range is selected (in the example, it is 40%) and the critical region (shown by the blue dashed lines) is established as a function of AR1. c. A confusion matrix is prepared and the number of false alarms and well-predicted LDs are determined. The procedure in b. and c. is repeated for several ranges of critical region. d. The ideal critical region range is established when the initial linear trend (shown in red) is disrupted, since a further increase in the range yields a lower value of the ratio of false alarms to well-predicted LDs.

- It is possible to connect points that share the same point density by generating rainfall frequency contour lines (RFCLs). These lines represent a measure of the frequency of occurrence of the rainfall events and may be used as threshold lines to assess how the magnitude of the rainfall events influence landslide occurrence.
- Rainfall-induced landslides, in principle, should occur due to high-magnitude rainfall events whose daily and/or antecedent rainfall rarely occurs in the analyzed environment. On the other hand, those landslides that are said to have been triggered by a rainfall pair that lies close to the origin (i.e ordinary rainfall combinations) are very likely to have occurred due to a major contribution from anthropogenic disturbances.

Figure 10 summarizes the procedure employed to construct the RFCLs. For every day in the study period, the antecedent rainfall for 1, 2, 3 and 4 days is determined and 4 rainfall pairs are established. For each antecedent rainfall duration, a daily vs. antecedent rainfall plot is prepared with the respective rainfall pairs (Figure 10a). A buffer having a radius of 5 mm of rainfall is drawn around each rainfall pair (Figure 10b). The number of rainfall pairs falling within each buffer is determined and this number is then divided by the area of the buffer to obtain the point density (Figure 10c). Rainfall pairs having the same point density are joined by the RFCL (Figure 10d).

For the distinction of LDs and NLDs, the RFCLs sharing the same *point of origin* were merged into *threshold sets*. The point of origin of a RFCL can be defined as the point where the contour line intersects the y-axis. In each daily vs. antecedent rainfall plot, nine points of origin were marked along the y- axis: the same number of RFCLs were drawn at 5-mm intervals between 5 and 45 mm of daily rainfall along this axis. Due to the resemblance, third order polynomials were fitted to all 9 RFCLs in each plot to ease the evaluation of the lines as thresholds (see Figure 11). Threshold sets were then created by joining the 4 RFCLs that have the same point of origin in the plots. As an example, the point of origin of the RFCL in Figure 10 is 37 mm; it is possible to establish a threshold set by merging this RFCL with the other three lines having a point of origin at 37 mm for 1, 3 and 4 days of antecedent rainfall.

Finally, the predictive performance of each threshold set was determined. The fitted polynomials, which are expressed in terms of actual antecedent rainfall, yield 4 minimum triggering rainfall values required for landslide occurrence for each day in the study period. The lowest of these values is then compared to the actual daily rainfall of that day to determine threshold exceedance. In this way, the number of well-predicted LDs (i.e. days in which the threshold was exceeded and a landslide occurred) and the number of false alarms (i.e. days in which the threshold was exceeded, but no landslide occurred) for each set was calculated.

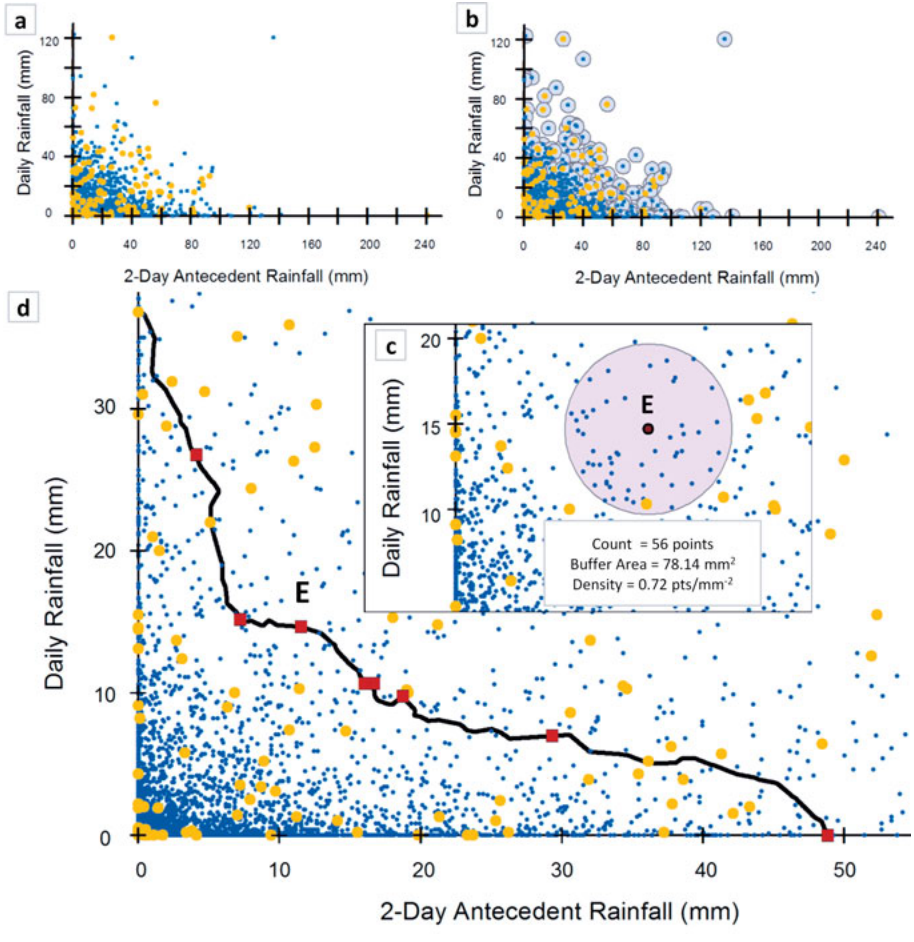

Figure 10. Procedure to draw a RFCL with a point density magnitude of 0.72 for a 2-Day Antecedent Rainfall. **a** LDs (orange dots) and the NLDs (blue dots) are plotted in the daily vs. 2-day antecedent rainfall graph; **b** The 5 mm-rainfall buffers are drawn around all points; **c** The point density magnitude is determined. As an example, for point E, the point density magnitude is calculated by dividing the number of points within its buffer by the area of the buffer; **d** a black RFCL is drawn to connect point E with 7 other red squares whose point density magnitude is equal to 0.72. This RFCL has a point of origin of 37 mm (i.e. the RFCL intersects the y-axis at 37 mm)

4.3 Spatial analysis

4.3.1 Comparison between event-based inventories

In **Paper I**, the database´s coverage of landslides triggered by Hurricane Mitch in October of 1998 has been evaluated by means of a comparison with two event-based inventories that have been derived from aerial photo-

graph interpretation. These are: a) the inventory developed by the USGS, based on an aerial photograph taken in March of 1999 (Harp et al., 2002), and b) the inventory developed by JICA for major landslides, based on an aerial photograph survey carried out between mid-February and mid-May of 2001 (JICA, 2002). This comparison has highlighted the limitations of press archives as sources of landslide spatial data, which were explored more in detail during the construction of the study area´s susceptibility maps.

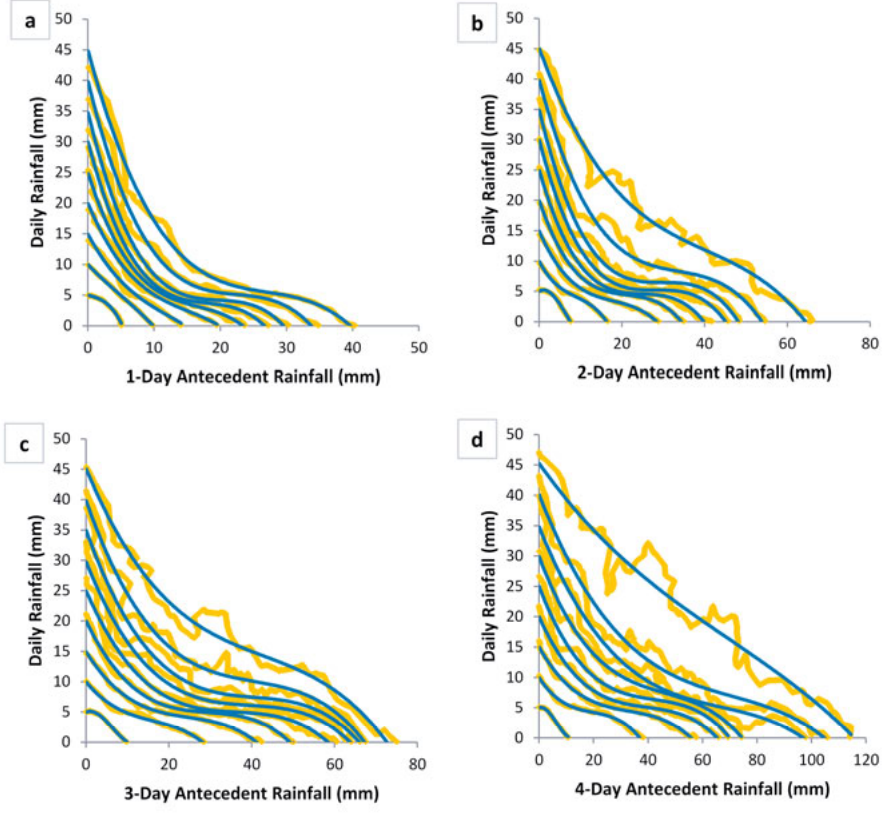

Figure 11. For all 4 daily vs. antecedent rainfall plots, 9 RFCLs are shown in orange. These RFCLs originate at 5, 10, 15, 20, 25, 30, 35, 40 and 45 mm of rainfall along the y-axis. The blue lines are 3rd order polynomials that have been fitted to the corresponding RFCLs. a. 1-day antecedent rainfall; b. 2-day antecedent rainfall; c. 3-day antecedent rainfall; d. 4-day antecedent rainfall.

4.3.2 Susceptibility mapping

Paper IV evaluates the press archives as a data source for landslide susceptibility mapping at a local scale. Figure 12 shows an overlay of the two inventories used to construct two susceptibility maps. On the one hand, land-

slide polygons resulting from aerial photograph interpretation performed in 2014 by JICA experts (Yamagishi et al., 2014) were used to construct the Aerial Photograph Interpretation susceptibility map (hereafter known as the API map). On the other hand, a map of landslide-affected neighborhoods (or unstable neighborhoods) derived from the press-based database has been used to construct the Press-Based susceptibility map (hereafter known as the PB map). It is worth mentioning that a neighborhood map of the city was used for the construction of the map of landslide-affected neighborhoods. If a landslide was documented in the news reports as occurring in a specific neighborhood, then the entire neighborhood was considered as affected by the landslide, regardless of the size of the landslide. This approach was followed because it was usually possible to locate the landslides in the neigh-

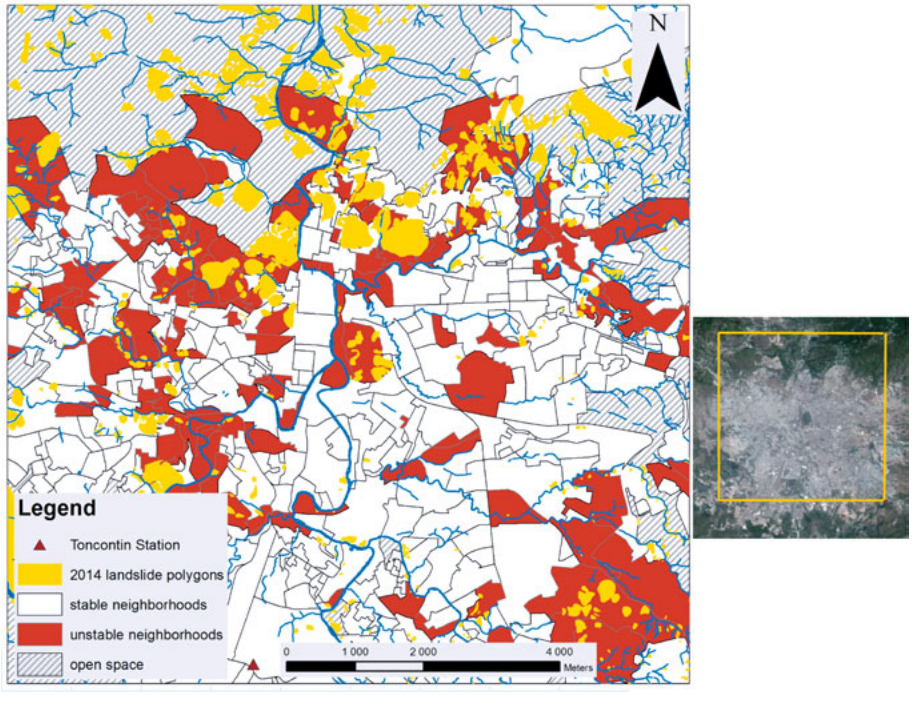

Figure 12. The two landslide inventories used to assess the spatial occurrence of landslides. The yellow polygons show the landslide bodies inventoried through the aerial photograph interpretation from 2013 to 2014 (Yamagishi et al., 2014). The white and yellow polygons show the stable and unstable neighborhoods during the 1980-2005 period respectively, according to the press-based database. The hatched polygons depict the open areas present in the study area in 2001 (JICA, 2002). The orange border overlaying the Google image of Tegucigalpa (to the right) shows the actual area analyzed.

borhood map but the scarcity of spatial information provided by the press archives regarding the extent and boundaries of the landslide impeded a more accurate delimitation.

For this analysis, three environmental variables –slope angle, geology and distance to drainage- were chosen due to their significant contribution to landslide occurrence in the study area. Slope angle is the most important factor in any landslide analysis, as it provides the potential energy that drives the downward movement of rock, soil or debris material while the slope reaches a more stable position (Cross, 1998). Concerning geology, despite the fact that very few physical tests have been performed to characterize the geological units in the study area, previous studies have shown that some geological units in the study area exhibit a higher propensity to slope failure than others (Harp et al., 2009; JICA, 2002; Yamagishi et al., 2014). Meanwhile, the distance to drainage has been considered an important factor in other landslide study areas (Akgun et al., 2008; Lee & Sambath, 2006; Süzen & Doyuran, 2004) and in the case of Tegucigalpa, it has been demonstrated that the undercutting of river banks has triggered several landslides in the past (e.g. during the passage of Hurricane Mitch (Harp et al., 2002)).

The data source for the selected variables was a thorough and detailed field study carried out by JICA experts in 2001 after the passage of Hurricane Mitch in 1998 (JICA, 2002):

- Slope angle: JICA's topographic map, with contour lines at 2.5 meter-intervals, was used to construct a triangulated-irregular network (TIN). This allowed the computation of the slope angle for every pixel in the study area using ArcGis. The fact that only 8 % of the study area had slopes greater than 30° served as a guideline for the creation of seven classes; the last class particularly covers these steep slopes.
- Geology: JICA's geologic map of the city, at a scale of 1:10,000, shows that Tegucigalpa is composed of Valle de Angeles formations in the Cretaceous period, the Matagalpa formations in the Paleogene period, the Padre Miguel group in the Tertiary period and Quaternary volcanic deposits. This map contains 21 different geologic units.
- Distance to drainage: As part of the flood analysis, JICA conducted a detailed survey that allowed the generation of spatial data for the four major rivers and streams of the city. Four buffers having a width of 50 meters each and covering a distance of 200 m on each side of the rivers and streams were created.

The spatial assessment of landslide occurrence was carried out using the matrix method, which calls for fewer variables than other statistical methods and therefore, is ideal for data scarce regions (De Graff et al., 2012). Each

variable was then divided into different classes (see Table 5). The two landslide inventories and the three environmental factors were converted into raster images in ArcGis for the easiness in spatial data management. The study area, which has a size of 100 km^2, was divided into a grid of 50 x 50 meter pixels and a total of 40,000 pixels were created. Each pixel stored information regarding the presence or absence of landslides using both inventories as well as information concerning the explanatory variables. Unique Condition Units (UCUs) (Clerici et al., 2002) were then created to represent unique combinations of three classes, one for each explanatory variable.

Table 5. *Classes of explanatory variables*

Variable	Classes	Variable	Classes
Geology	1. Tcg	Slope Angle	1. 0-5°
	2. TM		2. 5-10°
	3. Qal		3. 10-15°
	4. River bank		4. 15-20°
	5. Qe3		5. 20-25°
	6. Qan1		6. 25-30°
	7. Qan2		7. >30°
	8. Tpm3		
	9. Qe1	Distance to Drainage	1. 0-50 m
	10. Krc		2. 50-100 m
	11. Qe2b		3. 100-150 m
	12. Qb		4. 150-200 m
	13. Tpml		5. >200 m
	14. Qe2a		
	15. Kvn		
	16. Tpm2		
	17. Tpm1		
	18. Tep		
	19. Reservoir		
	20. Odt		
	21. Ti		

In each of the susceptibility maps, the Landslide Susceptibility Index (LSI) was calculated as

$$LSI_{UCU} = \frac{number\ of\ pixels\ in\ landslide\ cells\ in\ a\ given\ UCU}{total\ number\ of\ pixles\ in\ the\ UCU}. \qquad (6)$$

A higher value of LSI indicates a higher susceptibility to landslides. To complete the susceptibility map, five susceptibility classes were created in each map using the Natural Breaks classification method built in ArcGIS. Figure 13 summarizes the employed methodology to construct the susceptibility maps.

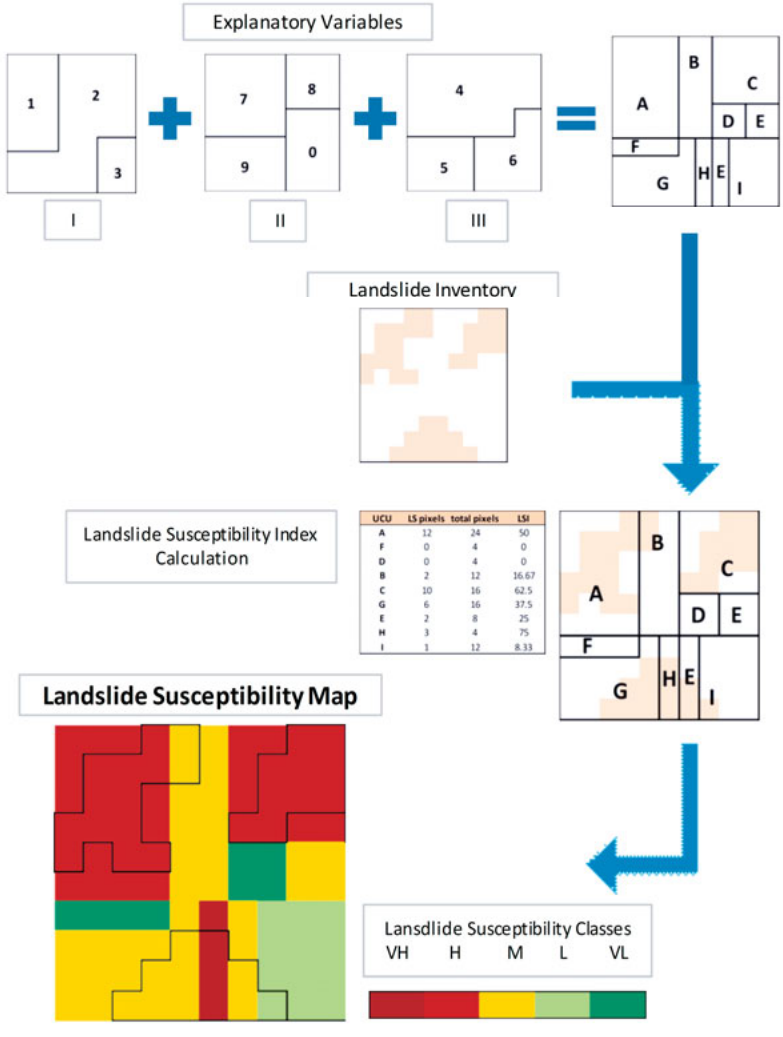

Figure 13. Methodology scheme for the construction of the susceptibility maps

Success and prediction rate curves were prepared to evaluate the general performance of the susceptibility maps (Bui et al., 2013; Zêzere et al., 2004). Two success rate curves were obtained by comparing each landslide susceptibility map with the respective landslide inventory used for the map construction. The prediction rate curve, on the other hand, was obtained by determining how well the PB susceptibility map predicted the 2014 landslide polygons, which were not used in any sense during the construction of the PB susceptibility map. To be able to understand why the PB map had a low predictive performance in identifying the 2014 landslide polygons, these polygons were then separated into 3 categories depending on their location within the PB landslide inventory: Group A contained those landslide poly-

gons within landslide-affected neighborhoods, Group B contained all those polygons within stable neighborhoods and Group C contained all those polygons within the open spaces of 2001. An additional prediction rate curve was constructed to determine how well the PB susceptibility map predicted the landslide polygons in Group A.

Finally, a pixel by pixel comparison of both susceptibility maps enabled the determination of the percentages of correct and acceptable classification as well as the percentages of susceptibility underestimation and overestimation. Süzen & Doyuran (2004) have proposed that an acceptable classification involves pixels that are either correctly classified (i.e. they share the same susceptibility class in both maps) or have only one susceptibility class difference between the two maps (e.g. from "very high" in one map to "high" in the other). Meanwhile, considering that the API map yields a more reliable representation of the study area's susceptibility, susceptibility overestimation occurs when a pixel in the PB map has a higher susceptibility class than in the API map. Likewise, susceptibility underestimation occurs when a pixel in the PB map has a lower susceptibility class than in the API map.

5. Results

5.1 Database Compilation

Paper I reveals that the database currently contains 393 rainfall-induced landslides that have occurred between 1980 and 2005, yielding an average of approximately 15 landslides per year. An additional 7 landslide entries that have been referred to in the scrutinized press archives and therefore compiled into the database, have been excluded from this analysis, as these have taken place before 1980. The number of landslide events used in the temporal and spatial analyses is specified in the corresponding section, as it is not possible to reconstruct the antecedent rainfall conditions for all 393 landslides or locate them all on the available neighborhood map of the city.

5.2 Temporal Analysis

5.2.1 Annual and Monthly Scale

Figure 14 shows the annual rainfall and landslide distribution for the 26-year study period. The red line represents the five-year moving average of landslides per year. It can be seen that the lowest averages occur at the beginning of the study period, while the highest concentration of landslides takes place in the years between 1995 and 1999 (hence, the maximum value in the year 1997). Despite the slight decrease in the moving average after Hurricane Mitch in 1998, a general increase in the number of landslides per year with time is evident. Although the proliferation of the population living in areas vulnerable to landslides may partly account for this increasing trend, the social perception of landslides has been progressively enhanced (especially after Hurricane Mitch) and this has lowered the minimum threshold required to document landslides in the press.

Eighteen of the 393 landslides contained in the database lack information regarding the month of occurrence. Because their incidences have been reported in the first three or four days of a month, there is uncertainty whether the landslide occurred in the previous month or the one in which it has been reported. Figure 15 shows the influence of the rainfall seasonality on the occurrence of the 375 landslides considered for this analysis. While September is the wettest month of the year (155.44 mm of rainfall on average)

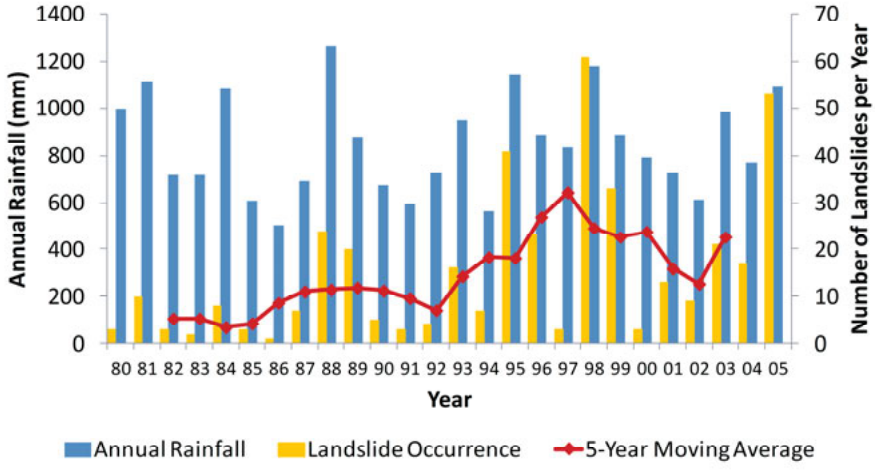

Figure 14. Temporal distribution of landslides on a yearly basis. The blue bars correspond to the annual rainfall (primary vertical axis). The orange bars correspond to the number of landslides that have taken place each year (secondary vertical axis). The red line shows the 5-year Moving Average.

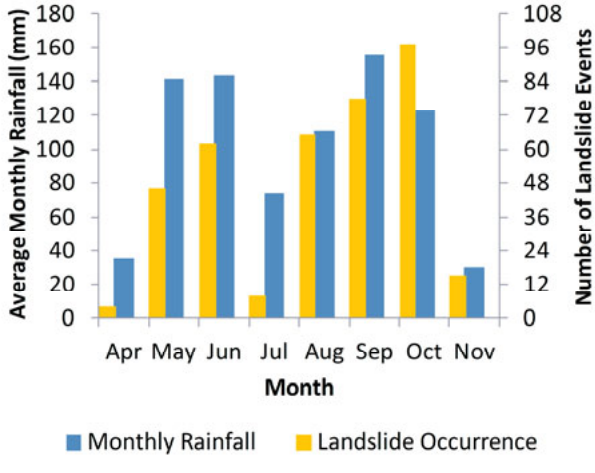

Figure 15. Influence of rainfall seasonality on landslide occurrence. The blue columns correspond to the Average Monthly Rainfall (primary vertical axis). The orange columns correspond to the number of landslides that have taken place during those months (secondary vertical axis).

and has the second highest incidence of landslides (78 in total), the substantial contribution of landslides triggered by Hurricane Mitch ranks October as the leading month in landslide occurrence (97 in total, 30 attributed to the hurricane), despite this month's average rainfall is the fourth largest with

123.18 mm per month. In contrast, the occurrence of the Mid-Summer Drought in July (Alfaro, 2002) may account for such a low incidence of landslides during this month (8 in total).

In relation to the initiation of landslides in April and November, although the average rainfall in these months is very similar (35.55 mm and 30.25 mm respectively), the number of landslides in the former month is nearly one fourth of those taking place in the latter month (4 and 15 respectively). This reveals that the different soil formations of Tegucigalpa can provide an adequate response to rainfall infiltration during April when the terrain is completely dry (i.e. at the beginning of the rainy season), but may reach failure with easiness in November when the formations' strength is low as a result of saturation (i.e. at the end of the rainy season).

Finally, it is possible to establish a monthly rainfall threshold for landslide occurrence. All months were plotted in a graph having the monthly rainfall in the x-axis and the number of landslides in the y-axis. Figure 16 shows that for monthly rainfall values greater than 240 mm, there has always been at least one landslide occurrence. The red line serves as a threshold for minimum landslide occurrence. As an example, if 300 mm of rainfall are recorded, a minimum of 9 landslides are expected.

5.2.2 Rainfall thresholds

Paper II shows that the construction of rainfall thresholds has been conducted on the 244 events for which the day of occurrence has been clearly stated or can be easily derived from the press archives. Figure 17a shows that for 65 of the 244 landslides considered, the exact time of initiation is known; for an additional 23 events, the time of the day (e.g. early morning, morning, afternoon, evening) has been acknowledged. For the remaining 156 landslides, only the day of landslide occurrence has been provided in the news reports. In addition, Figure 17b shows that while 93 landslides have occurred as single events, there have been 3 major rainfall events that have been capable of triggering between 9 and 20 landslides almost simultaneously.

5.2.2.1 Critical Rainfall Intensity

Table 6 shows the 12 LDs of 1998 and the respective CRI values based on threshold duration. As an example, the most critical antecedent condition for the LD of the 28th of October for the 7 days prior to landslide occurrence (i.e. the antecedent duration extends from 1 to 7 days) took place on the 7th day. However, when the 7-day time window of TH07 has been widened to include the antecedent conditions for 9, 12 and 15 days prior to landslide occurrence, the antecedent rainfall amount of 15 days yielded a higher return period. Finally, whether the 30 days (TH30) or the 60 days (TH60) prior to

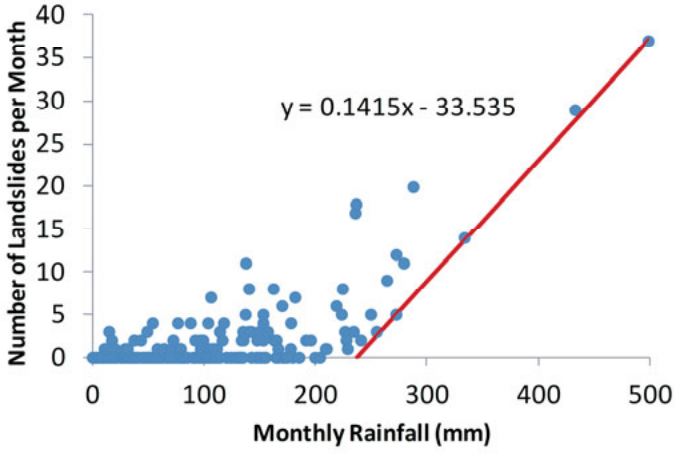

Figure 16. Monthly threshold (red line) indicating the minimum number of landslides based on the monthly rainfall.

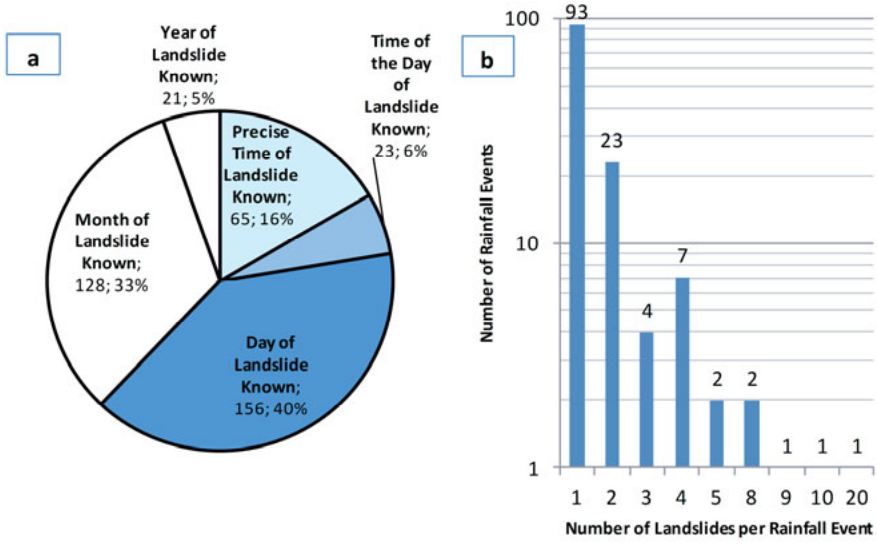

Figure 17. a. Pie graph showing the temporal detail of landslide occurrence for all events in the database. The portions of the graph with blue shades contain a total of 244 landslides, occurring in 134 days. b. Bar graph showing the number of landslides per rainfall event vs. the number of rainfall events. It can be seen that while most landslides occurred as single events (i.e. 93 rainfall events have triggered one landslide each), three rainfall events have triggered 9, 10 and 20 landslide respectively.

Table 6. *Selection of the CRI based on the threshold duration (LDs of 1998)*

LD	Threshold Duration											
	TH07			TH15			TH30			TH60		
	AD (day)	AR (mm)	CRI (mm/ day)	AD (day)	AR (mm)	CRI (mm/ day)	AD (day)	AR (mm)	CRI (mm/ day)	AD (day)	AR (mm)	CRI (mm/ day)
24 May	-	-	-	-	-	-	-	-	-	-	-	-
1Jun	4	121.2	30.3	9	182.6	20.3	9	182.6	20.3	9	182.6	20.3
9 Jul	3	23.6	7.9	3	23.6	7.9	26	93.2	3.6	50	195.9	5.9
28 Aug	3	46.4	15.5	3	46.4	15.5	3	46.4	15.5	3	46.4	15.5
5Oct	3	35.4	11.8	3	35.4	11.8	3	35.4	11.8	60	271.5	4.5
14 Oct	1	17.5	17.5	12	97.3	8.1	12	97.3	8.1	55	298.0	5.4
15 Oct	2	34.3	17.1	15	114.2	7.6	22	143.0	6.5	60	323.1	5.4
22 Oct	1	30.1	30.1	15	138.6	9.2	22	185.3	8.4	60	362.5	6.0
27 Oct	7	63.2	9.03	15	139	9.3	26	217.9	8.4	60	348.7	5.8
28 Oct	7	76.4	10.9	15	151.7	10.1	26	231.5	8.9	26	231.5	8.9
30 Oct	3	40	13.3	15	143.7	9.6	30	257.9	8.6	30	257.9	8.6
1 Nov	2	240.7	120.3	2	240.7	120.3	2	240.7	120.3	2	240.7	120.3

AD = Antecedent Duration; AR = Antecedent Rainfall; CRI = Critical Rainfall Intensity, obtained by dividing the AR by its corresponding AD; LD = Landslide Day. For the LD on 24th of May, none of the antecedent rainfall amounts yielded a return period greater than 1.

the LD are considered, the most critical antecedent rainfall took place during the 26 days prior to landslide occurrence.

Figure 18 shows the four threshold arrays[1]: TH07, valid for 7 days; TH15, valid for 15 days; TH30, valid for 30 days and TH60, valid for 60 days. Each plot in Figure 18 consists of all LDs (represented by diamonds), the mean CRI for each antecedent duration (represented by triangles) and 3 parallel lines: the uppermost Line A, which underlies 15% of all LDs; the thin and central Line B, constructed on the basis of the mean CRI of each antecedent duration and whose regression equation is shown; and the lowermost Line D, which underlies 85% of all LDs. Line C has been omitted from all plots as these lie very close to Line B.

[1] For the purpose of this thesis, a threshold array defines the four threshold lines belonging to a specific threshold duration. For example, TH07A, TH07B, TH07C and TH07D all constitute the TH07 threshold array. In **Paper II**, this array was referred to as a threshold set, but this term has also been employed in **Paper III** to refer to the threshold RFCLs that share the same point of origin. For example, the four lines that originate at 37 mm along the y-axis of all 4 daily vs. antecedent rainfall graphs constitute the THS37 (see Figure 23).

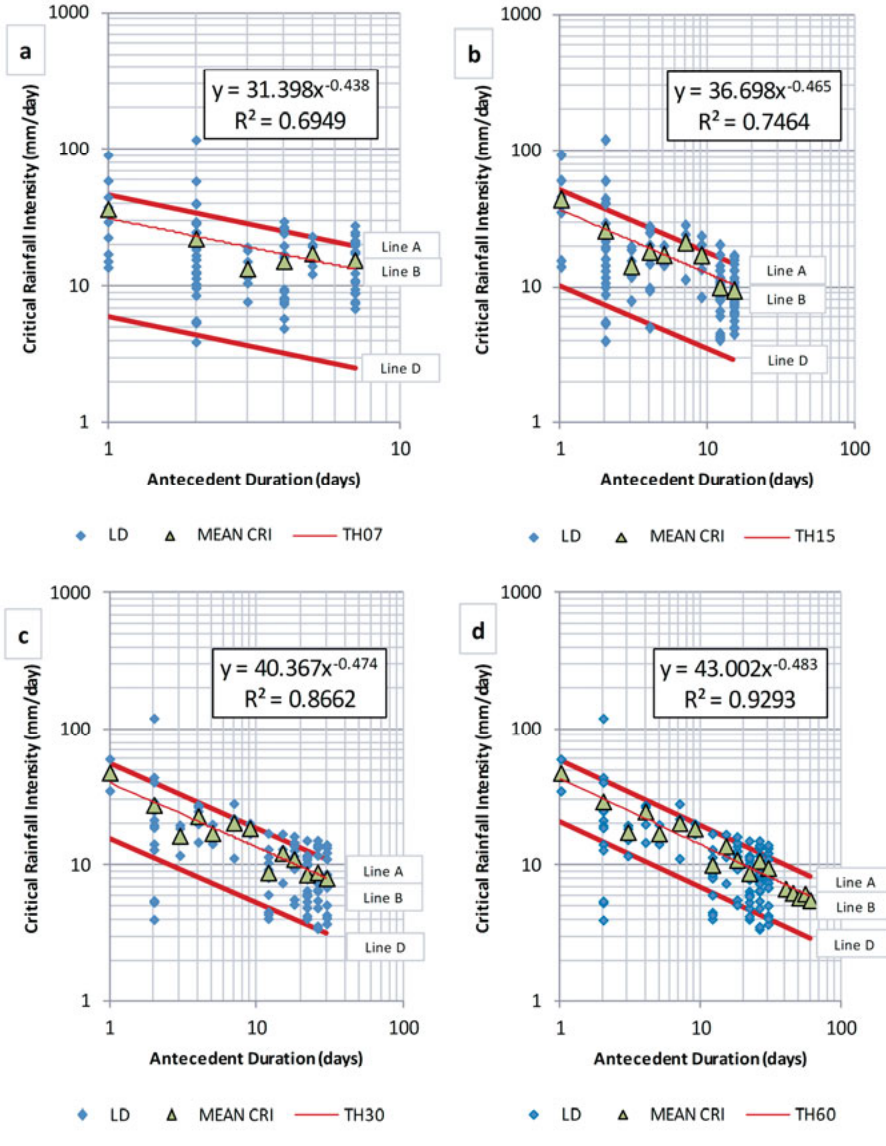

Figure 18. Four threshold arrays for the four analyzed threshold durations: A) TH07, valid for 7 days, B) TH15, valid for 15 days, C) TH30, valid for 30 days and D) TH60, valid for 60 days. Each threshold array contains three lines: Uppermost Line A underlies 15% of all LDs, central Line B, constructed on the basis of the mean CRI (green triangles) for each antecedent duration and whose regression results are shown in the corresponding box; Lowermost Line D underlies 85% of all LDs.

Figure 19 displays the performance of all 16 threshold lines in the ROC space. The shape of the points is unique to every threshold duration: squares corresponds to all TH07 lines, diamonds to TH15 lines, circles to TH30 lines

and triangles to all TH60 lines. As well, different colors are associated to every level of accuracy in predicting LD: red correspond to the four Line A thresholds, blue to the Line B thresholds, yellow to the Line C thresholds, and green to the four Line D thresholds. From Figure 19, it is evident that the variability of the FPR tends to increase as the number of well-predicted LDs increases: all Line A thresholds are clustered together relatively close to the origin (see the lower enclosed image), while the biggest dispersion corresponds to the Line D thresholds, which lie high above the line of random fit (shown in orange) and not far from perfect classification. Furthermore, whether Lines A, C or D are considered, the TH07 lines (shown by the squares) always exhibits the lowest FPR values, indicating that all TH07 lines yield the least false alarms when 15%, 50% and 85% of all LDs are well-predicted. For this reason, TH07 was explored further (hereafter known as Modified TH07) to allow: a) the integration of the triggering rainfall into the threshold, and b) the determination of the best TPR-FPR relationship that can maximize the predictive performance of LDs with the least number of false alarms.

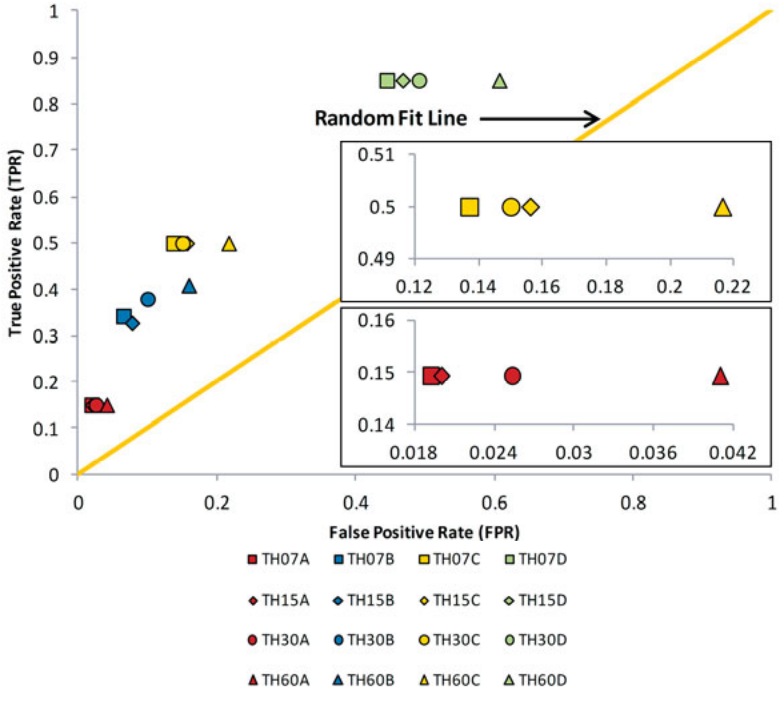

Figure 19. Performance of the 16 threshold lines in the ROC space. The shape of the points is unique to each threshold duration. Color varies with Lines A, B, C and D. A close-up of the relative position of the 4 Line A and 4 Line C threshold lines (red and yellow points, respectively) is also presented. The line of random fit is shown in orange.

Figure 20 shows the plot for the Modified TH07, which integrates the triggering rainfall into the threshold. In this graph, LDs whose triggering rainfall amounts yielded higher return periods than any of its antecedent rainfall amounts, are plotted as orange dots on the line $x = 0.1$. It can be seen that Lines A and D (uppermost and lowermost red lines) encompass the majority of the LDs whose CRI is related to the triggering rainfall (29 in total); an additional 8 LD lie below Line D while only 1 LD falls above Line A. The fact that nearly one-third of all LDs (38 out of 134, or 28.4%) are significantly affected by the triggering rainfall shows that when the analysis of LDs is limited to the antecedent conditions only, the unnoticed contribution of the triggering rainfall may lead to a false attribution of landslide occurrence to ordinary antecedent rainfall episodes. This explains why the performance comparison of Lines A, C and D of the Modified TH07 with respect to the TH07 reveals that a lower number of false alarms have occurred in the former threshold to correctly predict 15%, 50%, and 85% of all LDs: 109 vs. 124, 768 vs. 851 and 1912 vs. 2787, respectively.

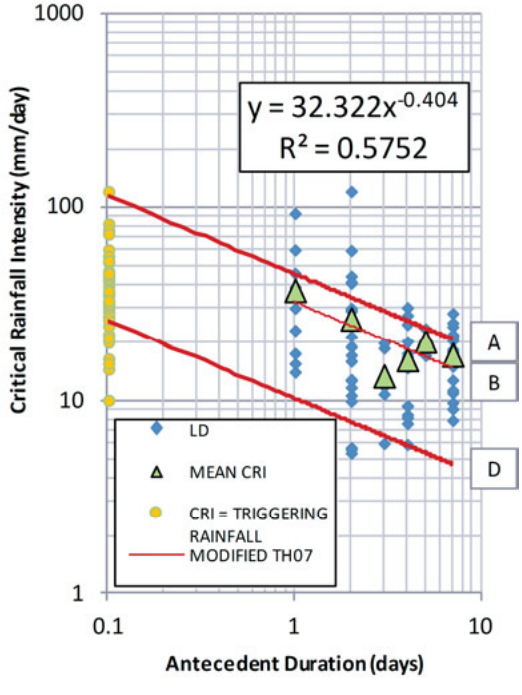

Figure 20. Plot for the modified TH07, which includes the triggering rainfall (represented as yellow dots) as the CRI of several LDs. These have been plotted on the line x = 0.1. Green triangles represent the mean CRI upon which the regression line (thin red line, also known as Line B) has been constructed. Uppermost and lowermost bold red lines are Lines TH07A and TH07D respectively.

The analysis of the ratio of false alarms to well-predicted LDs with respect to the range of the critical region (explained in Figure 9) showed that the best results in terms of reduction of false alarms are obtained when the critical region extends to 82% of the antecedent rainfall amounts dictated by the threshold. The number of well-predicted LD is lowered to 88 (i.e. 83% of the 106 LDs provided by the threshold without the critical region), yet the number of false alarms has substantially decreased to 902 (i.e. nearly 55% of the 1622 false alarms provided by the threshold without the critical region). Despite the fact that the *r* value has increased to 0.373, the number of false alarms required to yield one well-predicted LD is also substantially reduced to 10 (i.e. a reduction of 33% with respect to the 15 yielded by the model without adjustment). Therefore, the proposed rainfall threshold for the city of Tegucigalpa, Honduras for the period 1980 to 2005 is

$$I = 12.2D^{-0.40}, \tag{7}$$

where D ranges from 0.1 to 7 days and the Critical Region covers an additional 82% of the antecedent rainfall amount dictated by the same threshold. Table 7 gives a summary of the three stages of the TH07.

Table 7. *Summary of the stages of TH07*

Parameter	TH07	Modified TH07	Modified TH07 with Critical Region (range = 82% of Antecedent Rainfall)
a	10.2	12.2	12.2
b	-0.44	-0.40	-0.40
Well-predicted LDs	106	106	88
False alarms	1932	1622	902
WPLDs / FA	18.2	15.3	10.2
r	0.375	0.335	0.373

To illustrate the effectiveness of the Critical Region, Figure 21 shows a plot of triggering vs. antecedent rainfall for an antecedent duration of 5 days for the months of August and September of 1988. During these months, a total of 10 LDs were recorded (shown as red squares), of which 8 of them lie above the red threshold line. While 12 false alarms have occurred, the inclusion of the critical region (shown as the rectangle in dashed lines) has disregarded 13 days that fulfilled the antecedent rainfall requirements but failed to meet the requirements imposed for the triggering rainfall. Similar plots can be constructed for the remaining antecedent days.

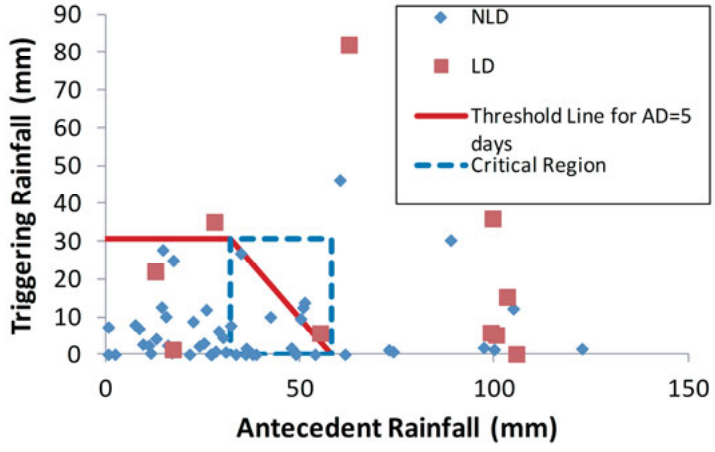

Figure 21. Example of the effectiveness of the Critical Region in reducing false alarms. The blue diamonds represent NLDs during the months of August and September 1988. Red squares represent LDs while the red line shows the threshold line for an antecedent duration of 5 days. The Critical Region, which is shown as the rectangle in dashed lines, covers 82% of the antecedent rainfall amount. A total of 13 days have fallen below the threshold line within the Critical Region and are therefore considered as negatives by the model.

5.2.2.2 Rainfall Frequency Contour Lines

The construction of RFCLs has been conducted in the daily vs. antecedent rainfall plots for 1, 2, 3 and 4 antecedent days. Apart from having a point density magnitude, all RFCLs also have a point of origin that corresponds to the intersection of the RFCL and the y-axis in each of the plots. Figure 22 shows how the point density magnitude of the RFCLs varies with the daily rainfall at the point of origin for all 4 antecedent rainfall durations. The 4 log-log plots reveal 3 different linear behaviors. The breaks between the lines in these plots are considered ideal for the establishment of a two-bound threshold: rainfall events falling below the lower bound (i.e. daily rainfall of 7 mm in all plots) are not likely to trigger landslides unless there has been a major anthropogenic disturbance, while rainfall combinations falling above the upper bound (i.e. daily rainfall between 37 and 40 mm) are rare, high magnitude events with the potential to trigger landslides without the influence of other contributing factors. Rainfall events falling between these two bounds may trigger landslides with some influence of anthropogenic disturbances. The establishment of a threshold based on the intersection of fitted correlation lines in a log-log plot was also suggested by Li et al. (2011) when analyzing the cumulative frequency of landslides and rainfall magnitude in the Zhejiang province in China.

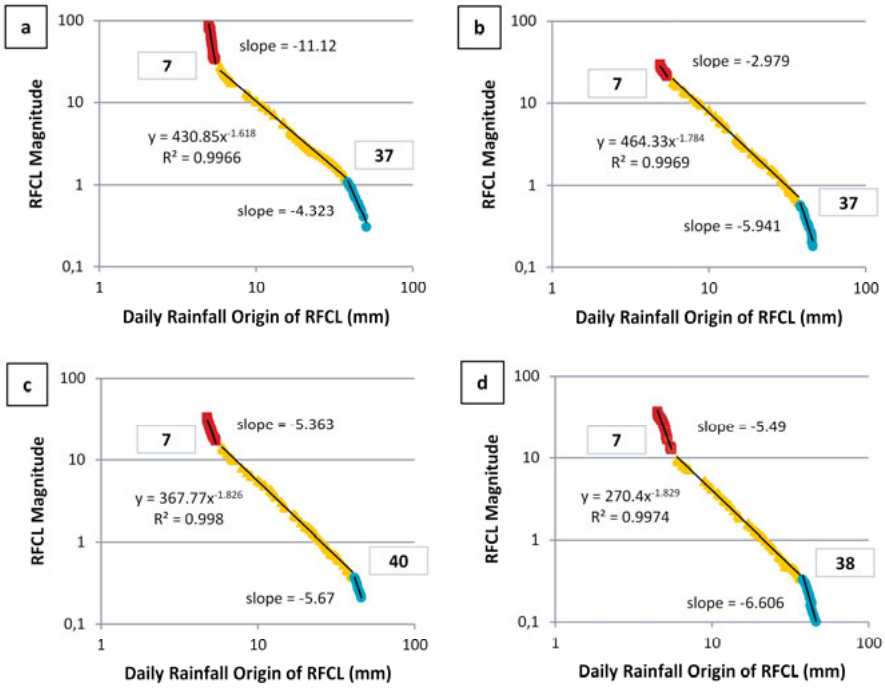

Figure 22. Log-log plots showing the behavior of the RFCLs point density magnitude with respect to the daily rainfall origin of the RFCLs. The number in the boxes show the daily rainfall value at which the breaks between the lines occur. a. 1-day antecedent rainfall. b. 2 day-antecedent rainfall. c. 3-day antecedent rainfall. d. 4-day antecedent rainfall.

The RFCLs having the same point of origin in the 4 plots have been grouped together into threshold sets. The threshold sets shown in Figure 23 correspond to the 4 RFCLs having the points of origin at a) 7 mm (THS07) and b) 37 mm (THS37). Due to their shape, third order polynomials have been fitted to all RFCLS to ease the evaluation of the lines as thresholds. For a given day in the study period, the equations for THS07 yielding the minimum triggering rainfall for landslide initiation ($minTR$) based on the actual antecedent rainfall (AR) for all antecedent durations (e.g. 1D stands for 1-Day antecedent rainfall) are as follows

$$minTR_{07\,1D} = -0.00547 * AR_{1D}^3 - 0.02104 * AR_{1D}^2 - 0.32526 * AR_{1D} + 7 \quad (8\text{-a})$$

$$minTR_{07\,2D} = -0.00263 * AR_{2D}^3 + 0.04654 * AR_{2D}^2 - 0.52986 * AR_{2D} + 7 \quad (8\text{-b})$$

$$minTR_{07\,3D} = -0.00085 * AR_{3D}^3 + 0.03376 * AR_{3D}^2 - 0.52898 * AR_{3D} + 7 \quad (8\text{-c})$$

$$minTR_{07\,4D} = -0.0004 * AR_{4D}^3 + 0.01781 * AR_{4D}^2 - 0.36884 * AR_{4D} + 7. \quad (8\text{-d})$$

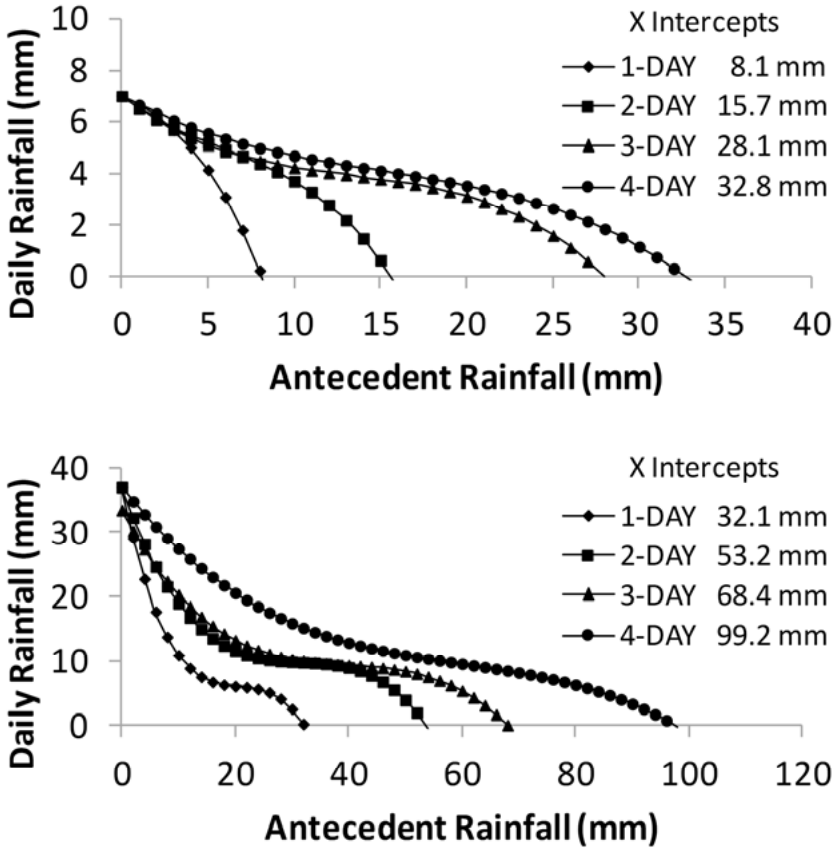

Figure 23. The RFCLs originating at 7 mm and 37 mm along the x-axis in all 4 antecedent duration plots are merged to constitute two threshold sets respectively: a) THS07 and b) THS37. The symbols represent the antecedent duration: diamonds represent the 1-Day antecedent duration, squares represent the 2-Day antecedent duration, triangles represent the 3-Day antecedent duration and circles represent the 4-Day Antecedent duration.

Likewise, the equations yielding the minimum triggering rainfall for landslide occurrence for THS37 are as follows

$$minTR_{37\,1D} = -0.00333 * AR_{1D}^3 + 0.20653 * AR_{1D}^2 - 4.34662 * AR_{1D} + 37 \text{ (9-a)}$$

$$minTR_{37\,2D} = -0.00082 * AR_{2D}^3 + 0.07787 * AR_{2D}^2 - 2.50486 * AR_{2D} + 37 \text{ (9-b)}$$

$$minTR_{37\,3D} = -0.00034 * AR_{3D}^3 + 0.04282 * AR_{3D}^2 - 1.85865 * AR_{3D} + 37 \text{ (9-c)}$$

$$minTR_{37\,4D} = -0.00009 * AR_{4D}^3 + 0.01631 * AR_{4D}^2 - 1.11304 * AR_{4D} + 37. \text{(9-d)}$$

For the latter threshold set, it is implied that if no antecedent rainfall occurs within 4 antecedent days, a daily rainfall amount of 37 mm would still be enough to trigger a landslide. This critical value is slightly greater than the one found in **Paper II** (the critical triggering rainfall was 30.6 mm) but is similar to the 39-mm daily rainfall proposed by Kirschbaum et al. (2012) for the Central American region.

Table 8 exemplifies the use of Equations 9-a to 9-d for the analysis of 12 LDs that took place in 1988. For a LD to be well-predicted, its daily rainfall must be greater than or equal to at least one of the *minTR* calculated based on its 4 antecedent rainfall amounts. For each day, the bold cells indicate the antecedent condition, if any, in which the daily rainfall exceeds the minimum triggering rainfall for landslide occurrence. This means that if a row has at least one bold cell, then the LD has been well-predicted by the threshold set. Overall, Equations 9-a to 9-d accurately predict 10 out of the 12 LDs and only 2 missed alarms have been produced. Table 8 also shows that more LDs are well-predicted when the conditions of several antecedent days are considered. Had the single ideal antecedent duration been 1 or 4 Days, only 7 LDs would have been well-predicted. If the ideal antecedent duration would have been 2 or 3 days, only 6 or 8 LDs would have been well-predicted, respectively.

Table 8. *Performance of THS37 for Landslide Days of 1988*

Date	Daily Rainfall (mm)	Antecedent Rainfall (mm)				Minimum Triggering Rainfall (mm)				Well-predicted LD?
		1-Day	2-Day	3-Day	4-Day	1-Day	2-Day	3-Day	4-Day	
12 Jun	20.4	60.2	66.5	76.6	76.6	**0**	**0**	**0**	**7.0**	Yes
25 Aug	35.1	6.2	7	10	20.1	**17.2**	**23.0**	**22.3**	**20.5**	Yes
26 Aug	5.7	35.1	41.3	42.1	45.1	**0**	8.6	9.3	11.7	**Yes**
29 Aug	0.1	46.2	58.7	64.4	99.5	**0**	**0**	4.1	**0**	Yes
30 Aug	36	0.1	46.3	58.8	64.5	36.6	**6.6**	**6.6**	**8.9**	Yes
31 Aug	5.2	36	36.1	82.3	94.8	**0**	9.5	**0**	1.4	Yes
10 Sep	22	2.4	5.1	12.8	12.8	27.7	26.1	**19.5**	25.2	Yes
15 Sep	82	13.8	13.8	13.8	40.6	**7.6**	**15.1**	**18.6**	**12.7**	Yes
18 Sep	5.8	1.8	3.3	85.3	99.2	29.8	29.5	**0**	**0**	Yes
20 Sep	15.3	12.2	18	19.8	21.3	**8.6**	**12.3**	**14.3**	**19.8**	Yes
27 Sep	1.3	2.4	11.2	15.7	15.7	27.7	17.6	17.0	23.2	No
5 Nov	1	0	25.3	25.3	25.3	37	10.1	11.8	17.8	No

Bold cells indicate conditions in which the daily rainfall of each LD exceeds the minimum triggering rainfall amounts, which have been determined based on the antecedent rainfall for all 4 antecedent durations. If the minimum triggering rainfall is equal to 0 (e.g. for 1, 2, and 3 antecedent days for LD of 12 Jun), it means that a landslide may be expected even if there is no triggering rainfall on that day. The antecedent rainfall values for such days are greater than the x intercepts shown in Figure 23b.

Table 9 shows the number of well-predicted LDs, false alarms, missed alarms and well-predicted NLDs for the threshold sets between THS07and

THS40. It can be seen that while THS07 has the highest number of well-predicted LDs (i.e. 116), it also produces the highest number of false alarms (i.e. 1883). This indicates that the predictive power of this threshold set is very low since 31% of all days are plotted above the RFCLs that constitute the threshold set without a proper distinction between LDs and NLDs. It can be seen that the rainfall combinations of 18 LDs (approximately 13% of all LDs contained in the database) constitute false alarms because these have fallen below the lines of THS07. With respect to the threshold set of the upper bound, the RFCLs of THS37 underlie 81 days in which landslides were reported and an additional 521 days in which no landslide occurred, yielding approximately 6 false alarms for every well-predicted LD.

Table 9. *Performance of threshold sets in distinguishing between days with and without landslides*

Threshold set	Well-predicted LD (WPLDs)	False Alarms (FAs)	Well-predicted NLD	Missed Alarms	FAs/WPLDs
7[a]	116	1883	4327	18	16.23
10	112	1634	4576	22	14.59
15	108	1319	4891	26	12.21
20	101	1094	5116	33	10.83
25	97	892	5318	37	9.2
30[b]	89	722	5488	45	8.11
35	82	574	5636	52	7
37[c]	81	521	5689	53	6.43
40	76	458	5752	58	6.03

a = The RFCLs that constitute THS07 have been proposed in **Paper III** as the boundary under which LDs are very likely to occur only due to a high contribution of anthropogenic actions.
b = THS30 allows the comparison of the landslide predictive performance yielded by the RFCLs method and the one proposed in **Paper II** using the same dataset.
c = Above the RFCLs of THS37, LDs are likely to occur due to rare, high-magnitude rainfall episodes without the need of any other contributing factor.

Table 9 suggests that the method described in **Paper III** constitutes an improvement in the predictive performance of the previous threshold line presented in **Paper II** for the same dataset. With the inclusion of the critical region, the Modified TH07 accurately predicted 88 LDs; yet, with the occurrence of 902 false alarms, approximately 10 false alarms are produced for every well-predicted LD (see Table 7). Meanwhile, the threshold set THS30 derived in **Paper III** relatively produces the same number of well-predicted LDs (i.e. 89) with a reduced number of false alarms (i.e. 722, 180 less than the previous method) and consequently, the ratio of false alarms to well-predicted LDs is lowered to 8. In essence, the latter method has made possible a 20% reduction of false alarms.

5.3 Spatial Analysis

5.3.1 Event-based inventory

Figure 24 shows a combined map of the inventories developed by JICA, the USGS and the press-based database for Hurricane Mitch in October of 1998. Particular focus is given to the northern area of Tegucigalpa (see enclosed image) where the majority of landslides were triggered by the hurricane. It can be seen that the pink polygons with red borders, which represent the neighborhoods affected by landslides according to the press-based inventory, have a fair agreement with the dark red polygons (from the USGS inventory) and the orange-striped polygons (from JICA). A total of 6 and 22 neighborhoods from the press-based inventory have agreement with the landslides mapped by JICA and the USGS, respectively. In addition, two more neighborhoods coincide with the brown polygons showing the possible areas affected by landslides, according to JICA (2002). This supports the statement that the damage-oriented perspective of press archives makes it difficult to distinguish between source and deposition areas of landslides and consequently, only the area where the damage occurs is usually reported. Overall, the comparison between the press-based inventory and the inventories based on aerial photograph interpretation has confirmed the landslide damages occurring in 24 of the 35 neighborhoods reported in the press archives, yielding a 69% of reliability.

From Figure 24, it is evident that unlike the maps developed from aerial photo interpretation, the press-based inventory lacks a desirable spatial resolution that allows the determination of the exact location of the landslides, making it difficult to estimate landslide characteristics such as run-out distances and areal extent. In addition, given that press archives tend to present only those landslides that have caused significant damage to the population, those landslides occurring in the open space polygon in the northernmost part of the map (shown in gray) as well as many other minor landslides, have not been documented. As discussed in **Paper IV**, this becomes a major issue in the construction of landslide susceptibility maps that limits the reliability of press archives as sources of landslide spatial data. Therefore, when evaluating disastrous events like Hurricane Mitch, the high costs of undergoing an aerial survey may be justified by the abundance of detailed spatial data that can lead to a better understanding of the unusual episode.

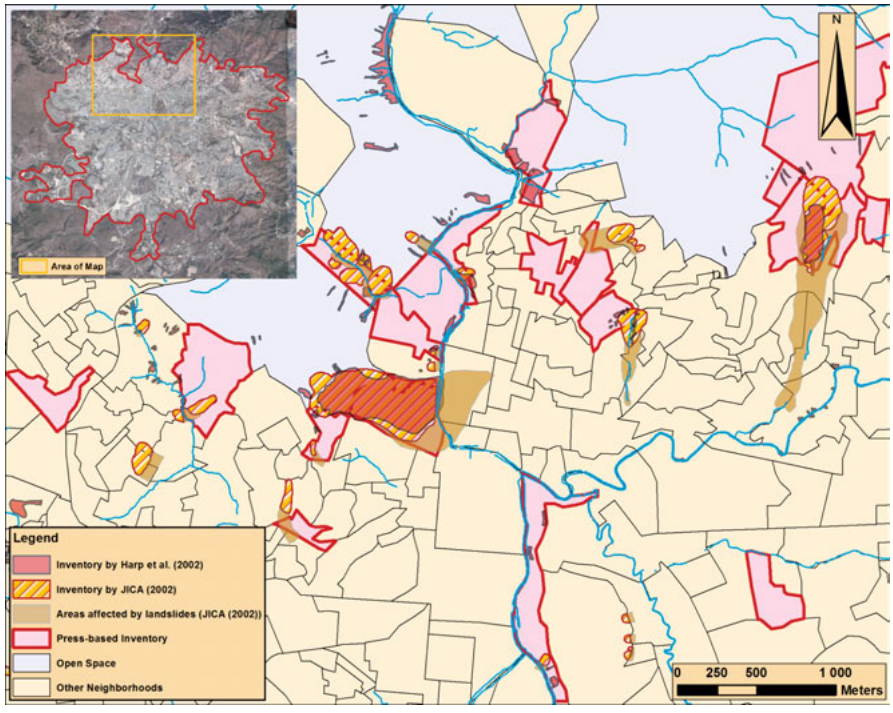

Figure 24. Comparison map for three landslide inventories developed for Hurricane Mitch in October 1998. The dark red polygons represent landslides mapped by Harp et al. (2002). The striped orange polygons depict those landslides recognized by JICA (2002); brown polygons accompany these landslide polygons to show the possible area affected by the displaced material. The pink polygons with red borders represent those neighborhoods affected by landslides reported in press archives. Gray and yellow polygons represent open space and other neighborhoods, respectively.

The main advantage that the press-based inventory has over the inventories based on aerial photograph interpretation is the relatively-rich temporal detail that makes it possible to indicate if particular landslides have been active within a certain period of time. As seen in Figure 14, the year of 1998 was considerably wet and several neighborhoods affected by the landslides mapped through aerial photograph interpretation suffered damages as early as June while many others were active at the beginning of October (i.e. before the occurrence of the hurricane). Thus, it is hard to distinguish solely from the photograph interpretation if the copious rainfall of the hurricane actually initiated the landslides or barely triggered reactivations.

5.3.2 Multi-temporal inventory

The reliability of press archives in the construction of a landslide susceptibility map for the 1980-2005 period is addressed in **Paper IV**. Of the total 393

landslide events found in the database, 309 landslides (79%) were successfully found in the neighborhood map provided by (JICA, 2002) and a landslide-affected neighborhood map was constructed to serve as the press-based landslide inventory. These landslide-affected neighborhoods occupy an area of 23.5 km^2. Unfortunately, it was not possible to locate the remaining 84 landslides because either these were referenced to places not available in the neighborhood map (49 cases), these occurred along major roads with no additional spatial reference (24 cases) or these were vaguely referenced to places involving more than one neighborhood, like the El Berrinche Hill (11 cases), as described in **Paper I**. In addition, an inventory based on an aerial photograph interpretation done in 2014 by JICA experts has also been used to construct a second landslide susceptibility map (Yamagishi et al., 2014).

Figure 25 shows the two landslide susceptibility maps prepared for each of the inventories. The landslide-affected neighborhoods (Figure 25a) and the 2014 landslide polygons (Figure 25b) are marked by gray borders to provide a visual overview of the consistency between the color associated with the different susceptibility classes and the absence/presence of landslides in the pixels. As expected, the API map is able to capture the 2014 landslide polygons within the high (orange) and very high (red) susceptibility classes more precisely than the PB map does with the landslide-affected neighborhoods. In addition, while the PB map depicts an apparent stable area towards the northeast of the study area, precisely where no landslides have been reported in the media and where the 2001 open spaces are located, the API map shows that this area is mainly moderately to highly unstable. Overall, even though the PB map seems to overestimate the landslide susceptibility of the area (i.e. it shows a higher presence of moderately unstable pixels than the API map), both maps seem to fairly agree that the areas delimited by the white-border ellipses are the most susceptible to landslides.

Figure 26a and Figure 26b show the success rate curves for both susceptibility maps. The results of the area calculation under these two curves confirm that the API map has a better general performance in identifying the landslide pixels used for its own construction than the PB map (80% vs. 68% respectively). In addition, the high score of the API map is a clear indication that the selected environmental factors are closely related to the occurrence of past landslide events in the study area. On the other hand, Figure 26c reveals that the general predictive performance of the PB susceptibility map is relatively poor when the landslide polygons identified in 2014 were used for its validation: the area under the prediction rate curve is barely 57%.

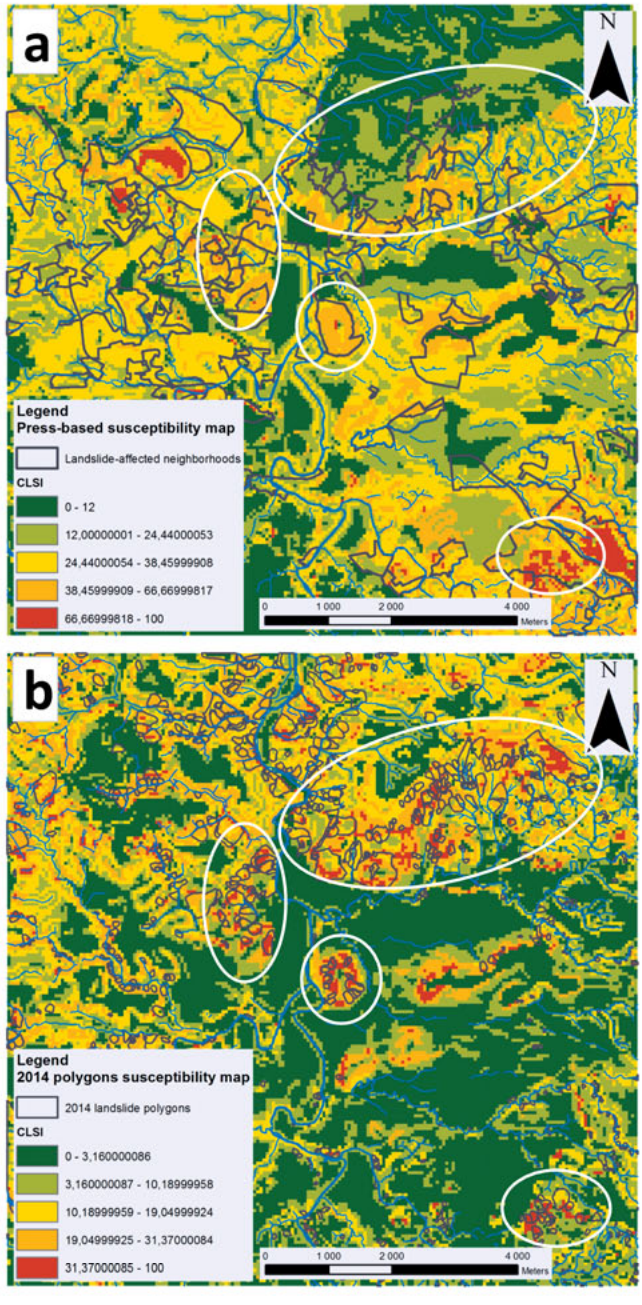

Figure 25. Landslide susceptibility maps: a. the press-based map and b. the aerial photograph interpretation map. The five susceptibility classes shown are very low (dark green), low (light green), moderate (yellow), high (orange) and very high (red). The landslide-affected neighborhoods and the 2014 landslide polygons are shown by the polygons with gray borders, respectively. The white-border ellipses show areas of higher susceptibility with a relatively good agreement between the two maps.

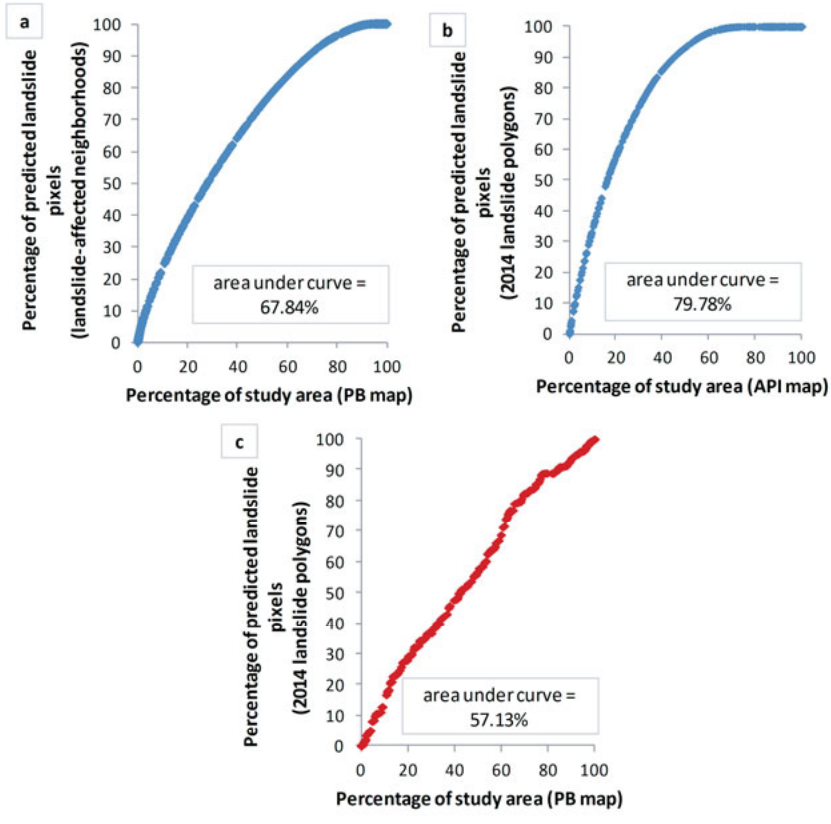

Figure 26. a. Success rate curve for PB susceptibility map based upon the landslide affected neighborhoods. b. Success rate curve for API map based upon the 2014 landslide polygons. c. Prediction rate curve for PB susceptibility map based upon the 2014 landslide polygons.

To be able to explain the PB map's low predictive performance, the 2014 landslide polygon pixels were divided into three groups according to their location within the study area: group A covered those landslide polygons in landslide-affected neighborhoods according to the PB map (unstable neighborhoods), group B included the ones in stable neighborhoods and group C took into consideration the ones that have occurred in the open spaces of 2001. The results, shown in Table 10, reveal that almost all landslide polygon pixels in the "very high" susceptibility class (i.e. 56 of 58 pixels) and nearly 3 quarters of those in the "high" susceptibility class are located in the unstable neighborhoods.

Table 10 also reveals that nearly 50% of the landslide polygon pixels in the "low" and "very low" susceptibility classes are located in the open space group. This means that 23.94% of all landslide pixels are incorrectly classified as having a "low" or "very low" susceptibility. It is clearly demonstrat-

ed that the lack of media coverage in the open spaces filters out an important portion of the landslides that occur in the study area and this, in turn, impedes a more reliable landslide susceptibility analysis if one relies exclusively upon the press-based inventory. This statement is supported by Figure 27, which shows that the area under the prediction rate curve considering only the landslide pixels belonging to group A (i.e. the blue line) is 10% higher than the prediction rate curve when all landslide polygons are taken into account (i.e. the red curve, which was also shown in Figure 26c). This observation makes it clear that the PB susceptibility map is significantly affected by the incompleteness of the inventory and therefore may not perform as well as the API map (i.e. the general performance is still 12% higher for the latter map).

Table 10. *Distribution of landslide polygon pixels according to their location in the press-based map*

Susceptibility Class (S.C.)	Total number of landslide pixels	Group A Unstable neighborhoods		Group B Stable neighborhoods		Group C Open Space	
		# pixels	% of S.C.	# pixels	% of S.C.	# pixels	% of S.C.
Very high	58	56	96.6	1	1.7	1	1.7
High	694	514	74.1	66	9.5	114	16.4
Moderate	1133	530	46.8	135	11.9	468	41.3
Low	1178	476	40.4	125	10.6	577	49.0
Very low	507	109	21.5	120	23.7	278	54.8

It is important to point out that lower predictive results were also expected from the PB map due to the difference in time between landslide inventories. On the one hand, the landslides between 2005 and 2014 may be visible in the aerial photographs but certainly, these are not present in the press-based database. On the other hand, Vranken et al. (2015) has recognized that in tropical countries, the rapid growth of vegetation due to favorable climatic conditions obscures the evidence of past landslides that could be present in aerial photographs. Therefore, some landslides occurring in the 1980s and contained in the database may no longer be visible in the aerial photographs of 2014.

The two susceptibility maps were compared pixel by pixel to establish the percentages of correct, acceptable and unacceptable classification. Table 11 reveals that in addition to the 11770 correctly classified pixels shown in bold, an additional 15185 pixels shown in the non-shaded boxes also have an acceptable classification. Among these, for example, are the 505 pixels that belong to the "high" class in the PB map and to the "very high" class in the API map. When there is a difference of more than one susceptibility class

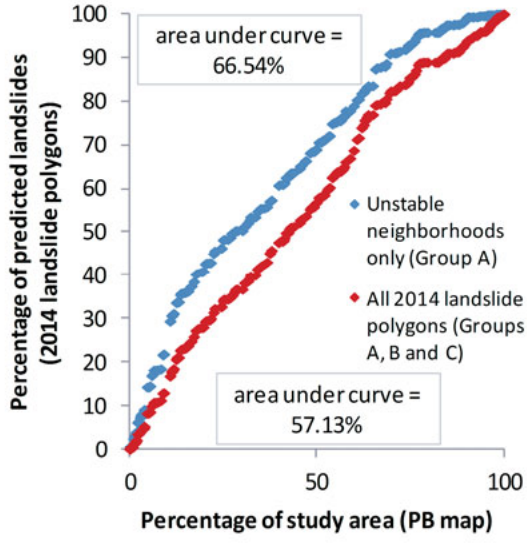

Figure 27. Prediction rate curve for the PB susceptibility map considering the 2014 landslide polygons in the unstable neighborhoods only (blue curve). The prediction rate curve considering all of the 2014 landslide polygons (red curve, same as in the Figure 26c) is shown as a mean of comparison.

Table 11. *Comparison of susceptibility classes between the PB map and the API map*

Aerial photograph interpretation map		Press-based map				
Suscepti-bility Class	Number of Pixels	Number of Pixels				
		Very high	High	Moderate	Low	Very low
Very high	1201	**98**	505	287	266	45
High	5678	5	**1457**	2041	1768	407
Moderate	7514	57	345	**1796**	3124	2192
Low	8988	109	1275	3611	**2626**	1367
Very Low	16617	344	1055	5238	4187	**5793**
Total	40000	613	4637	12973	11971	9804

Numbers in bold represent the pixels that have the same susceptibility class in both maps (i.e. correct classification). Non-bold numbers in non-shaded boxes represent pixels that are one susceptibility class away from a correct classification. For example, 505 pixels in the "high susceptibility class" of the PB map actually belong to the "very high" susceptibility class in the API map. On the other hand, the numbers in the shaded boxes represent pixels having an unacceptable classification because the susceptibility class to which they belong in one map is more than one class away from the susceptibility class in the other map. For example, 1275 pixels in the "high" class of the PB map are classified as "low" in the API map; this is an unacceptable classification because the difference in susceptibility classes is significantly high.

between maps (e.g. “very high” in one map and “moderate” in the other), the classification is regarded as unacceptable. All of these pixels are shown in the shaded boxes, including the 344 pixels that belong to the “very high” class of the PB map but to the “very low” class of the API map. Overall, it is shown that 29.43% of the pixels are correctly classified, 67.39% of the pixels follow an acceptable classification and 32.61% have an unacceptable classification.

Table 11 also enables the determination of the percentages of susceptibility overestimation and underestimation. Assuming that the API map shows a more reliable susceptibility representation of the study area, susceptibility underestimation occurs when a pixel in the PB map belongs to a lower suceptibility class than in the API map. Likewise, susceptibility overestimation occurs when a pixel in the PB map belongs to a higher susceptibility class than in the API map. Figure 28 shows that of the 67.39% of the pixels having an acceptable classification, 17.59% show susceptibility underestimation while 20.37% show susceptibility overestimation. In general, it is shown that the PB map tends to overestimate the susceptibility of the study area (i.e. 29.99% for underestimation vs. 40.57% for overestimation).

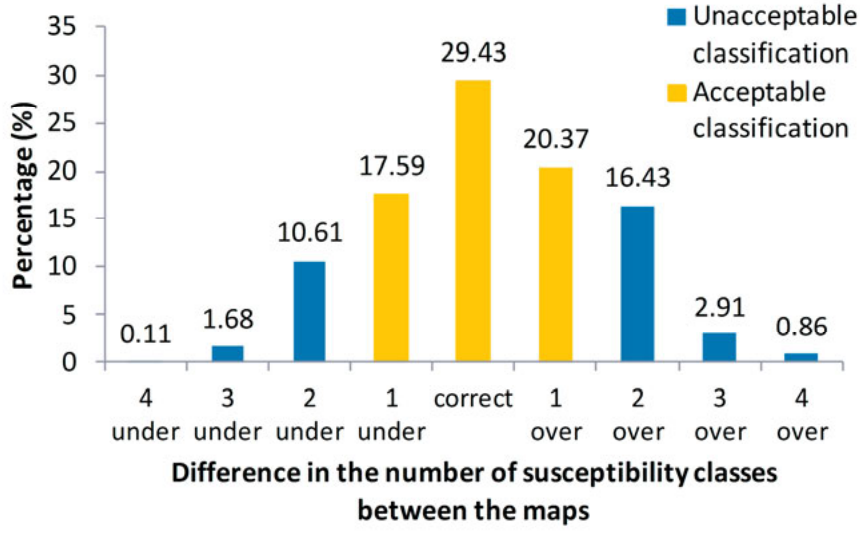

Figure 28. Bar graph showing the percentages of acceptable (orange columns) and unacceptable (blue columns) classification, as well as the percentages of susceptibility underestimation and overestimation

6. Discussion

6.1 The limitations, advantages and disadvantages of press archives

Several researchers worldwide have relied on press archives for the development of landslide databases (Devoli et al., 2007a; Domínguez Cuesta et al., 1999; Llasat et al., 2009). However, because press archives are seldom coming from a technical perspective, the data derived from them requires interpretation before it can be used in scientific analyses. As described in **Paper I**, the following situations limit the scientific richness of the database:

- the reporters' frequent use of qualitative adjectives that take the place of numerical parameters usually employed by scientists to characterize a landslide (e.g. descriptions of the size of a landslide as "big" or the intensity of a triggering rainfall as "very intense")
- the simultaneous occurrence of several landslides or landslides and floods, for which total damages are usually presented in the newspaper articles, usually being attributed to the triggering storm. This explains why the total landslide damages produced by Hurricane Mitch are underestimated in the database, as described in Section 5.3.1.
- the lack of training of the personnel documenting rainfall-triggered events, in identifying between landslides and floods. A similar situation led Guzzetti et al. (2005) to engage in a careful revision of the inventory for Italy, as it was found that several events that had been extracted from old reports and considered as landslides were actually floods.
- the reporters' tendency in recent times to rely significantly on images of the landslide rather than on descriptions when presenting the damages produced by the landslides

Raska et al. (2013) and Petrucci et al. (2009) emphasize that the crucial strength of newspapers relies on its capability of providing continuous information, enabling a reliable temporal analysis of landslide occurrence. The temporal richness of the 26-year database presented herein has allowed the construction of the rainfall thresholds described in **Papers II** and **III**. Such analyses have gained significance due to the limited availability of landslide temporal studies at the local and regional scale. First, the previous landslide studies in Tegucigalpa, as shown in Table 1, have provided little or no emphasis to the temporal aspect of landslide occurrence, probably owing

to the unavailability of relevant information in the past. Second, due to the limited rainfall records and landslide observations in Central America, few research teams have been able to establish rainfall thresholds in the region. To date, the Norwegian Geotechnical Institute has made threshold studies of lahars in Nicaragua and El Salvador possible (Nadim et al., 2009). Meanwhile, the National Aeronautics and Space Administration (NASA) has shown particular interest in the study of the triggering and antecedent rainfall conditions for landslide occurrence in the Central American region as part of a hazard model for evaluating potential landslide activity in near real time (Kirschbaum et al., 2015a). Certainly, the methods provided in these papers could be applied to other landslide prone areas in the region.

Unfortunately, the low spatial accuracy of the press archives may affect their use for spatial analyses. First, **Paper I** showed that the press archives were not able to capture all the landslide events that were evident in the aerial photographs used by the USGS and JICA for Hurricane Mitch. Second, **Paper IV** demonstrated that the aerial photograph interpretation done in 2014 provides a more reliable landslide inventory for the construction of susceptibility maps than the press archives. It is important to consider that the technique proposed to generate a press-based landslide inventory (i.e. assuming all pixels in landslide-affected neighborhoods as landslide cells) has certainly contributed to the susceptibility overestimation of the PB map with respect to the API map. Other approaches have been proposed to overcome the poor spatial location of landslides. For example, Klimes & Rios Escobar (2010) treated landslides as points rather than polygons, while Kirschbaum et al. (2015a) and Kirschbaum et al. (2015b) considered circular buffers surrounding the location provided in the media reports. In all cases, however, the authors have acknowledged that their methods may affect the reliability of the susceptibility maps, but these still provide acceptable results in highlighting the landslide-prone sites in the study areas.

6.2 The challenges of urban landslide studies

Petley (2009) has defined three different types of urban landslides: a) natural landslides that occur within an urban area, b) anthropogenically-induced landslides within an urban area and c) naturally or anthropogenically induced landslides that occur outside an urban area, but directly affect the urban population. The studies presented herein have disregarded those landslides occurring outside Tegucigalpa and have focused on both the naturally and anthropogenically induced landslides within the city. The difficulty of analyzing these landslides lies in establishing the degree to which the natural forces and human actions contribute to landslide occurrence.

As population pressure forces the urban boundary lines onto the hills of many major cities of the world (Schuster & Highland, 2007), human intervention is significantly contributing to the occurrence of many urban landslides. The anthropogenic disturbances cause loss of natural vegetation, undercutting and changes in the drainage patterns that alter the natural equilibrium of the environment and increase its susceptibility to landslides (Petley, 2009). In densely populated areas, even the smallest landslides demand significant attention due to the disturbances and losses (Chatterjea, 2011). Unfortunately, in many cities of Latin America, landslides usually affect the poorest sector of the population and lead to numerous deaths that could be prevented if urban planning codes were rigorously enforced to prevent development on slopes highly-susceptible to landslides (Alexander, 2005; Sepúlveda & Petley, 2015).

The challenges of analyzing urban landslides have been exposed in **Papers II** and **III**. First, urban areas are constantly evolving and therefore, within a short time span, the landslide susceptibility may increase (e.g. with the rapid development of slums on unstable slopes) or decrease (e.g. with the construction of mitigation structures such as retaining walls and surface water drains). This may also explain why it seems unrealistic to expect the PB susceptibility map described in **Paper IV** to account for all the 2014 landslide polygons. Second, low amounts of rainfall may appear to cause landslides in Tegucigalpa, but this occurs partly because anthropogenic activities have substantially predisposed the slopes to failure (Petrucci & Pasqua, 2009), therefore obscuring the real relationship between rainfall and landslides that would be evident in the studies of unused slopes. Consequently, researchers inevitably encounter major sources of uncertainty due to the difficulty in drawing a line between the effects of intense rainfall and man-made actions on the stability of slopes in urban areas (Chowdhury & Flentje, 2002). Third, many urban areas like Tegucigalpa are built upon active, slowly-moving landslides or landslide deposits (Antronico et al., 2013; Cascini et al., 2005), given that these areas have more gentle slopes that are ideal for the development of unplanned infrastructure. Unfortunately, the existing urban plans have failed to restrict development in these landslide sites and therefore, trying to establish the possible landslide triggers in populated and active environments becomes a more complex task.

6.3 Preparing Tegucigalpa for future landslides

Landslides should be seen as part of a natural process that require the efforts of the scientific community, local authorities, decision makers and the population in general to reduce their adverse effects on society. This is very important if one considers that the Central American region is expected to suffer an increase in temperature and a higher frequency of more intense precip-

itation events in the future (Aguilar et al., 2005). As an example, a time trend analysis using a global rainfall threshold as well as rainfall and landslide data for two volcanic study areas in Nicaragua (1958-2005) shows that the number of days exceeding the threshold as well as the intensity of the storms exceeding the threshold are increasing in time (Cepeda et al., 2010).

Based on the analysis of all four papers, the following are urgently needed to prepare the city for future landslide events:

- The establishment of a proper urban plan to control the population growth of the city and the areas available for development. In Central America, the current rate of urban growth is higher than in the rest of Latin America and this reflects a rural-urban transition that may bring negative consequences to the population living in major cities (UN-Habitat 2012). A recent study carried out in 2015 showed that Tegucigalpa currently has a deficit of 200,000 households (El Heraldo, 2015), indicating that the city is providing a home to more people than it can actually hold. As long as Tegucigalpa continues attracting the attention of the rural population, the uncontrolled growth will inevitably leads to the city's development in unstable areas, therefore increasing the susceptibility of the terrain to landslides.
- The establishment of a national geotechnical research unit whose main goal is to evaluate landslides as soon as they occur in order to provide technical evidence of the causes and mechanisms of the events. This will allow the enrichment of the landslide database with entries whose main trigger have been confirmed to be rainfall and will reduce the amount of uncertainties associated to the retrospective compilation of the database, as described in **Paper I**. It is likely that the performance of the rainfall thresholds and the PB susceptibility map may be diminished because landslide events significantly induced by manmade actions have been taken into consideration. Future landslide studies may yield more reliable results if such events are filtered out by the geotechnical research unit after a proper judgment of the causes and mechanisms associated with the failure.
- The deployment of additional rainfall stations in strategic places. On the one hand, rainfall measurements are essential for the issuing of warning and evacuation calls in landslide-prone areas. On the other hand, the study of Huggel et al. (2010) has shown that observation errors in rainfall measurements may lead to an exponential increase of losses due to landslides. Therefore, the investment in more rainfall stations is needed to improve the quality of the rainfall monitoring in order to provide more reliable alert calls when critical conditions have been reached. The susceptibility maps described in **Paper IV** may be useful to determine the location of these stations.
- An update of the rainfall threshold described in **Papers II** and **III**. One of the main components of an early warning system is the rainfall

threshold for landslide occurrence (Aleotti, 2004). Researchers working with rainfall thresholds have acknowledged that the exceedance of thresholds not always yields a landslide occurrence (Chleborad et al., 2006; Floris & Bozzano, 2008; Jaiswal & van Westen, 2009). Since false alarms emitted by early warning systems represent high economic and social costs to society (Huggel et al., 2010; Larsen, 2008), it is not feasible to produce a warning when the possibility of landslide occurrence is minimal. However, the case of the early warning system in Rio de Janeiro, Brazil suggests that the occurrence of new landslide events and the improvements in the rainfall data have led to an enhanced rainfall threshold for the city (Calvello et al., 2014). The thresholds described herein have been constructed using rainfall data from only one rainfall station, so it is possible to enhance their predictive power if new rainfall stations providing hourly rainfall are incorporated into the analysis.

- Prevention is a good way to reduce the negative effects of landslides. Fay et al. (2003) provides a clear example on how prevention has allowed Cuba to avoid serious damages from storms with similar magnitude as Hurricane Mitch. The prevention plan for Tegucigalpa should also include the proper training for the population living in landslide-prone areas. The study carried out between 2010 and 2012 by the United Nations Development Programme in 14 landslide-prone neighborhoods reveals that the population is not well informed on the causes of landslides and lack sufficient knowledge on the routines needed for evacuation in case of an imminent landslide (UNDP-DIPECHO, 2010, 2012)

All of the above indicate that society´s perspective towards landslides must be changed. The occurrence of Hurricane Mitch undoubtedly caused social awareness of the city's vulnerability to natural hazards. However, the occurrence of post-Mitch landslides on a yearly basis is a clear indicator that the city needs major actions to be taken. A recent landslide study in Latin America shows that during the 2004-2013 period, Honduras suffered 15 fatal landslide events in which 70 people lost their life. However, for this same period, only one academic paper for the country was found in the Web of Science database (Sepúlveda & Petley, 2015). Research is urgently needed as one of the first major actions to reduce the impacts of natural hazards in Tegucigalpa and the country in general. The findings of upcoming studies must be implemented in the future urban plans and emergency campaigns of the city. As long as the economic resources are destined to cover disaster losses and not invested for landslide studies, prevention or mitigation measures, the city will continue to suffer from landslides even during ordinary periods of rainfall.

7. Conclusions

In data scarce environments, press archives represent a valuable source of data that enables the temporal and, to a certain extent, the spatial analysis of landslides. While newspaper articles are focused on reporting the damages caused by landslides, important pieces of information can be recovered and used for scientific purposes. Part of the work presented herein has been destined to acknowledge the limitations of relying on press archives for landslide data and how these can affect the obtained results.

The major strength of press archives is the temporal richness of the landslide data. While aerial photograph interpretation and fieldwork allow detailed information for the precise moment of the survey, press archives may offer information for a wider temporal window, encompassing those landslides whose evidence of past occurrence may no longer be visible at the time of the survey. For this reason, significant effort has been granted to the construction of rainfall thresholds for landslide occurrence. Unfortunately, the urban nature of the landslides implies that anthropogenic disturbances have predisposed the slopes to failure and therefore, drawing a line between naturally induced landslides and those with some contribution of mankind still remains a challenge.

Due to the low spatial accuracy of landslides news reports, it has been shown that press archives may not perform as well as aerial photograph interpretation or other conventional sources used for landslide spatial analyses. Yet, the importance of showing how different a susceptibility map based on press archives is from that based on aerial photograph interpretation has been addressed. Where landslides have caused damage to society, a susceptibility map based on press archives may provide an acceptable measure of the terrain's proneness to landslides.

The papers discussed in this thesis along with the studies generated as a result of the passage of Hurricane Mitch in October 1998 provide a good overview of the landslide activity in Tegucigalpa, Honduras during the years 1980 and 2005. However, the current vulnerable situation of the capital city of Honduras in terms of landslides and floods requires immediate attention from the scientific community, local authorities and the population in general. Landslide risk management is an urgent necessity and must be integrated into the future urban plans of Tegucigalpa.

8. Future Work

Although the studies presented herein represent major steps towards the landslide risk management in Tegucigalpa, Honduras, there is still much more to be done. First, the current press-based database needs to be updated to incorporate major landslide events that have occurred in 2008, 2011 and 2013. This will allow a reevaluation of the rainfall thresholds proposed in this thesis. In addition, hourly rainfall data that has been generated in recent years may be considered for the construction of a new threshold that would enable a more accurate predictive performance in distinguishing between landslide and non-landslide days. As stated earlier, rainfall thresholds represent a major component in an early warning system, and although it is not possible to forecast all landslides, efforts should be directed to reduce the number of false alarms as much as possible.

Furthermore, although several landslide susceptibility maps for Tegucigalpa have been produced, the city currently lacks hazard and risk maps. The temporal and spatial analyses presented herein can be coupled to produce the first hazard map of the city. This will allow the determination of the probability of landslide occurrence in a given area of the city under given triggering and antecedent rainfall conditions. This hazard map coupled with a detailed study of the elements at risk under different landslide scenarios will eventually lead to the risk map of the city. The dissemination of the current and the future landslide studies will hopefully raise awareness of the need to start working towards the prevention of landslides and not limit the efforts to the disaster response once the landslides have occurred.

9. Acknowledgments

"To climb to the top of the mountain is your objective". That was all I knew when I started out my PhD studies. No map, GPS, or compass accompanied me to define my route. The slope was steep, the dense vegetation had many unpleasant surprises waiting for me and it was difficult to spot a marked pathway to follow. In my attempts to reach to the top, I was caught in several mudflows that brought me down to the bottom. During such moments of frustration, I realized it was easier to give up and seek an easy slope elsewhere. But I didn't. I had faith in God and He granted me everything I needed, in the right moment, to pursue my dream. Today, I am pleased to thank Him, in the first place, for never letting me down and for giving me the strength I needed to accomplish this endeavor. I also wish to thank all the people that, in one way or another, filled me up with motivation to continue, provided me with the energy for my journey, gave me advice on how to find the north whenever I got lost, rescued me when I had difficulties crossing the river, lifted me up when I had fallen and were there to cheer with me for every small step I took along my way towards the goal.

Thank you to the Swedish International Development Cooperation Agency (SIDA) and to the International Science Programme (ISP) at Uppsala University (contract number: 54100006) for their full support and for their interest in promoting science and capacity building in the Central American region.

Thank you to my supervisors Rafael Ferrera and Kennet Axelsson for your trust and for allowing me to discover my strengths and weaknesses as a young researcher. Thank you, Lars Christer-Lundin (R.I.P), because your positive attitude in difficult times always made me hope for a rainbow after a storm. Thank you, Sven Halldin, for the valuable opportunity to become part of the Centre for Natural Disaster Science (CNDS) research school and be able to continue with my investigation. Thank you, Kristofer Gamstedt, because you built up confidence in me and made me believe that I was capable of climbing to the top of the mountain. Thank you, Patrice Godonou, because your hard work, dedication and perseverance have always made you a role model for me. Thank you, Ernst van Groningen, for your guidance towards the end of my PhD.

I would also like to thank the staff member of the National Autonomous University of Honduras (UNAH) for their collaboration during my shorts

visits. Thank you, Deans Saul Jimenez and José Mónico Oyuela, for encouraging me to continue with my investigation despite the multiple limitations I had to face. Thank you to the Head of the Civil Engineering Laboratories, Marta Castro and to the Heads of the Civil Engineering Department, Carlos Murcia and Roberto Avalos, for providing me with a working space and access to the resources of our division. Thank you to Nabil Kawas and Lidia Torres from the Honduran Earth Science Institute (IHCIT) for the opportunity to collaborate with the ongoing landslide investigations.

It is my desire to express sincere gratitude to the Japanese International Cooperation Agency (JICA) for their valuable landslide investigations in Honduras since the occurrence of Huricane Mitch. Special thanks go to Hiromitsu Yamagishi, Masahiko Hayashi, Go Sato and Kiyoharu Hirota for sharing your knowledge and experience with me. In addition, I would like to thank Edwin Harp from the US Geological Survey (USGS) for providing me with data for one of my papers. Thank you, Katarina Lepp, for the outstanding landslide database app that you developed. It was a very useful tool to conduct my research. Thank you, El Heraldo newspaper, for the permission granted to use their images in my papers and in the thesis. I also want to express my profound gratitude to Bengt Lundberg, Cecilia Johansson and Anika Braun for your valuable time in reading my thesis and providing suggestions to improve it. Thank you, Arianna for making sure that some of my ideas were clearly written and could be easily understood. Thank you, Fritjof Fagerlund, for the help with the Swedish translation of the summary.

Thank you to Pravina, Zsuzsanna, Hossein and other staff members at ISP for ensuring my well-being during the latter part of my PhD. Thank you to all administrative and IT staff members at Geocentrum and Ångström for your fast and efficient service when it was needed.

Thank you to Team Honduras –José Luis, Zairis and Diana- for keeping the Honduran atmosphere alive in Uppis. It's always nice to eat baleadas, dance punta, and support our national football team while being away from home.

Thank you to the Central American community for the wonderful moments together. Agnes, Estuardo, José M., Beatriz, Tito and Eduardo, it has been a pleasure meeting you all and I am looking forward to collaborating with you in the future for the common good of the region.

Thank you to my officemates, Lebing, Liang, Adrian and Shahoui for always being there when I needed you. You always had the right words to make me feel good in difficult moments, and you were always the first ones to cheer my accomplishments.

Thank you to all my friends with whom I travelled in time to build medieval castles, grow crops in the Caribbean islands during the Spanish colonial period or explore a forbidden desert in search for a flying machine. David, Julio, Alejandra, Leo, Florian, Claudia, Oscar, Angela, Nilsa and Audrey,

thank you so much for always letting me be the Blue Meeple during our wonderful boardgame nights.

Thank you to my friends with whom I had a chance to explore fascinating places of the Old World. Enrique, Denis, Jinxing and Jinying, Ivon and Lars, thank you for the wonderful company and for the numerous Kodak moments during our trips together.

Chris, Nino, and Anna S, thank you for the tons of fun during this summer´s volleyball matches.

Daniela, Miriam, Stina, Erika L., Ida Å., Julia P. and Alexandra C., thank you for all our fikas together. I am grateful for your friendship during all these years.

To my friends who were once part of or are currently working at Geo, thank you so much for so many nice experiences during fikas, TGIFs, department dinners, and birthday celebrations. Ida W., Zhibing, Michael K., Alvaro, Peter D., Reinert, Carmen, Kristina C., Jean Marc, Marc, Kaycee, Martin, Anna K., Eva, Saba, Colin (from Peace and Conflict) and Leif, thank you for making me feel as part of the Geo family.

To my colleagues and friends at Ångström, Alexey, Juan José, Dan, Fengzhen, Åsa, Grim, Peter B., Nico, Urmas, Gaby, Andrea, Ingela, Marcus, Thomas, Sara, Reza and Sanjay, thank you for all these wonderful years packed with such nice social events. I cherish all the birthday celebrations, the afterworks, the summer grills, and the team-building trips. Thank you, Amra, for always cheering me up and for always emphasizing on the bright side of life. Esra and Bengt-Åke, thank you so much for the opportunity to collaborate during the laboratory sessions.

A mi Gordita Bella, Reina Isabel Urquía, has sido mi principal fuente de motivación durante todos estos años. Estar lejos de vos ha sido muy difícil, pero me ha ayudado muchísimo para valorarte aún más y darme cuenta que sos el tesoro más grande que Dios me ha dado. A mi padre Melquiades (Q.D.D.G), gracias por la buena educación que recibí de tu parte; además, valoro mucho que me hayas enseñado cuando niño a siempre cumplir con mis responsabilidades y a siempre dar lo mejor de mí porque ambas lecciones me impulsaron a terminar. A mi tía Vilma, gracias por todo su amor y comprensión durante todos estos años y por brindarle a mi madre la compañía que ella ha necesitado mientras yo he estado luchando por cumplir este sueño. Sin su ayuda, no tendría la dicha de estar escribiendo estas líneas.

A Aída Denisse, te agradezco por tu paciencia y amor durante todos estos años. Gracias porque siempre me has apoyado y porque has estado ahí cuando he necesitado de alguien con quien desahogarme, que me dé un consejo o para disfrutar de mis alegrías. Gracias también porque a tu lado, he aprendido a ser una mejor persona.

A mi Padrino Victor C, mi tía Carmen, mi tía Gloria, doña Argelia, mis demás tíos, primos y sobrinos en Honduras y Estados Unidos, gracias por

siempre pasar pendiente de mí. La distancia no ha sido impedimento para mostrarnos apoyo y cariño mutuamente.

A Kevin y a Ariadne, mil gracias por su valiosa ayuda en la recopilación de los archivos de prensa en las hemerotecas. Sin su colaboración, este proyecto no habría sido posible. Nunca olvidaré que en ese momento de dificultad, me tendieron la mano y me demostraron cuán importante es nuestra amistad.

A Laura, mil gracias por tus consejos, por siempre darme ánimo, por creer en mí y por todo tu cariño durante todos estos años de amistad. A mis amigos del Laboratorio de Suelos y Materiales, en especial a la Ing. Córdoba, al Ing. Matheu, a la Ing. G. Salgado, a Eric, Mario y Ramón, gracias porque cuando he estado de visita en Honduras, he sentido el mismo calor familiar que tuve antes de emprender mi primer viaje a Suecia. A Doris, Lourdes, Ada y Rita, gracias por su ayuda durante mis estadías.

Finalmente, a Vivian, Sadia, Alejandra L., Karen H., Blanca O. y Javier B., gracias porque durante todos estos años, me han demostrado su apoyo y porque el orgullo que sienten por mí ha sido una de mis principales fuentes de inspiración para luchar contra la adversidad en busca de alcanzar la meta.

10. Sammanfattning på svenska (Summary in Swedish)

Farliga naturhändelser kan utvecklas till naturkatastrofer särskilt när åtgärder saknas för att förhindra eller reducera negativa konsekvenser av sådana händelser. Tyvärr är effekterna av naturkatastrofer värre i utvecklingsländer. När det gäller Honduras, så har landets geografiska läge tillsammans med dess sociala, ekonomiska, politiska och kulturella sårbarhet bidragit till att det är ett av de mest sårbara länderna för naturkatastrofer. De omfattande skadorna som orsakades av orkanen Mitch i oktober 1998, ansedd som den mest förödande tropiska stormen under förra århundradet, avslöjade Tegucigalpas sårbarhet för jordskred och översvämningar. På grund av det begränsade antalet forskare inom geovetenskaper i landet och bristen på data från tidigare händelser, har det dock blivit en utmaning att analysera med vilken frekvens jordskred inträffar och de förutsättningar som krävs för att de skall ske.

Studierna som presenteras här har inriktats mot att visa användbarheten hos tidningsarkiv som värdefulla källor till data för jordskredsanalyser. Tillsammans med undersökningarna som utfördes efter orkanen Mitch, utgör dessa studier en grundlig genomgång av jordskred i Tegucigalpa, Honduras mellan 1980 och 2005. Tre huvudsakliga aspekter har behandlats: sammanställning av en databas samt temporär och rumslig analys av jordskreden. Den systematiska sammanställningen av data från tidningsarkiv och de metoder som använts här för att utvärdera data kan säkerligen användas också i andra områden eller miljöer som är utsatta för farliga naturhändelser och där brist på relevanta data råder.

I **Artikel I** presenteras metoden för att sammanställa databasen. På grund av den icke-vetenskapliga rapporteringen av jordskredshändelser i dagspressen, är det nödvändigt att belysa de huvudsakliga begränsningarna hos tidningsarkiv samt hur dessa kan påverka studier som baseras på denna typ av data. **Artikel I** klargör också att medan den stora styrkan hos tidningsarkiv är den temporala rikedomen i data, så kan den låga rumsliga noggrannheten påverka trovärdigheten. Artikeln tar fram korrelationer mellan jordskred och månatliga och årliga nederbördsdata. Vidare presenteras också en jämförelse mellan tre inventeringsmetoder: två av dessa sammanställdes efter orkanen Mitch och baseras på fältarbete och tolkning av flygfotografier medan den tredje baseras på tidningsarkiv som behandlar samma händelser.

I **Artikel II** används den temporala rikedomen hos tidningsarkiv för att analysera den prediktiva förmågan hos ströskelvärden med olika varaktighet för att särskilja dagar med och utan jordskred. Bestämmande-regnintensitetsmetoden användes för att skapa tröskelvärden med kort (7 dagar), medellång (15 dagar) och lång varaktighet (30 och 60 dagar). Metoden modifierades för att ta hänsyn till regnet som sätter igång ett jordskred. Studien visade att antalet falska alarm som erhölls med tröskelvärdena ökade när varaktigheten för tröskelvärdena förlängdes. Trots att en bestämmande period inkluderades för att öka den prediktiva förmågan hos 7-dagarströskelvärdet, så förblev antalet falska alarm per korrekt predikterat jordskred högt. Artikeln framhåller bidraget från mänsklig påverkan på att jordskred inträffar som en av utmaningarna vid analys av jordskred i urban miljö.

Artikel III föreslår en ny metod för framtagande av regntröskelvärden baserade på grafisk utvärdering av regnfrekvens. I detta fall analyserades grafer där igångsättande regn ritades mot tidigare inträffade regn för en fyra-dagarsperiod innan jordskredet inträffade. Regnfrekvenskonturlinjer ritades i graferna för att visa hur regnfrekvensen ändrar då dessa linjer ligger längre från origo. Metoden har två fördelar. För det första reducerades antalet falska alarm per korrekt predikterat jordskred med 20% jämfört med tröskelvärden för regnvaraktighet som användes i **Artikel II**. För det andra så möjliggjorde denna tvåfaldiga tröskelvärdesmetod att jordskred som framkallats på naturlig väg av regn kunde särskiljas från jordskred som hade krävt betydande mänsklig påverkan och destabilisering av sluttningar för att vanliga regnfall skulle kunna sätta igång dem.

Rumslig analys av jordskred behandlas i **Artikel IV**. De tre analyserade förberedande faktorerna var sluttningsvinkel, geologi och avstånd till floder. Två jordskredsbenägenhetskartor konstruerades med hjälp av matrismetoden: den första skapades från kartor över jordskredspåverkade områden som tagits fram från den 26-åriga tidningsarkivsbaserade databasen och den andra skapades från tolkningen av flygfotografier som gjordes 2014. Jämförelsen mellan de två jordskredsbenägenhetskartorna visade att kartan skapad från tolkning av flygfotografier bättre predikterade utbredningen av jordskredet 2014 jämfört med den tidningsarkivsbaserade kartan. Studien visade också att den låga prediktiva förmågan hos den tidningsarkivsbaserade kartan delvis beror på ofullständigheten i tidningarnas rapportering, vilken med säkerhet påverkades av avsaknad av nyhetsrapportering om jordskred i öppna områden. Överlag överskattades benägenheten för jordskred i staden av den tidningsbaserade kartan.

I den avslutande diskussionen presenteras en översikt över för- och nackdelar med att använda tidningsarkiv för analys av jordskred. Utmaningarna med jordskred i urban miljö diskuteras också. Vidare föreslås möjliga användningar av de studier som presenterats här för att bättre förbereda Tegucigalpa inför framtida jordskred.

11. Resumen en español (Summary in Spanish)

Las amenazas naturales se consideran desastres cuando no existe un manejo apropiado para la prevención y reducción de los efectos negativos de dichos eventos. Desafortunadamente, el impacto de los desastres naturales es mayor en países en desarrollo. En el caso de Honduras, su condición física acompañada de la vulnerabilidad social, económica, polítca y cultural de sus residentes, han contribuído para colocarlo como uno de los más vulnerables a desastres naturales. Los daños extensos causados por el paso del Huracán Mitch en octubre de 1998, considerada como la tormenta tropical más devastadora del siglo pasado, reveló la vulnerabilidad a deslizamientos de tierra e inundaciones del país, en especial de la capital y ciudad más importante, Tegucigalpa. Sin embargo, dado el número limitado de geocientíficos a nivel nacional y la escasez de datos relacionados a eventos pasados, el análisis de la frecuencia de deslizamientos de tierra y las condiciones físicas requeridas para la occurrencia de estos eventos se ha convertido en un reto.

Los estudios presentados en esta tesis han sido orientados a demostrar la utilidad de los archivos de prensa como fuentes de información para el análisis de los deslizamientos de tierra en Tegucigalpa. Al igual que las investigaciones realizadas después del acontecimiento del Huracán Mitch, estos estudios proveen una visión amplia de la actividad relacionada con los deslizamientos de tierra en la capital entre los años de 1980 y 2005. Tres aspectos importantes son abordados: la compilación de la base de datos y el análisis espacial y temporal de los deslizamientos de tierra. La recolección sistemática de información derivada de los archivos de prensa y los métodos empleados en los estudios para evaluar la información ciertamente pueden ser reproducidos en otros ambientes propensos a amenazas naturales y que se ven afectados por la escasez de información.

En el **Artículo I** se presenta el procedimiento aplicado para compilar la base de datos. Dado el enfoque no-científico de los reportajes acerca de los deslizamientos de tierra, es necesario destacar las limitaciones más importantes de los archivos de prensa y cómo éstas pueden afectar los estudios que se basan en dicha información. El **Artículo I** tambien deja claro que mientras la mayor fortaleza de los archivos de prensa es la riqueza temporal de información, su debilidad más destacada es la baja precisión espacial para

ubicar los deslizamientos. Este artículo provee correlaciones entre la ocurrencia de deslizamientos de tierra y la lluvia mensual y anual. Además, el artículo también proporciona una comparación entre tres inventarios de deslizamientos de tierra: dos de ellos recopilados después del Huracán Mitch y que han sido basados en trabajo de campo y la interpretación de fotografías aéreas y el tercer inventario derivado precisamente de archivos de prensa para este evento.

En el **Artículo II**, la riqueza temporal proporcionada por los archivos de prensa es explotada al analizar el desempeño predictivo de umbrales de lluvia de diferente duración en la distinción entre los días con y sin deslizamientos de tierra. Se utilizó el método de la intensidad de lluvia crítica para construir umbrales de corta (7 días), mediana (15 días) y larga duración (30 y 60 días). El método se modificó para incorporar la contribución de la lluvia detonante en la ocurrencia de los deslizamientos de tierra. Se demostró que el número de falsas alarmas brindadas por los umbrales aumenta con la duración de los umbrales. A pesar de incorporar una región crítica para mejorar el desempeño predictivo del umbral correspondiente a los 7 días, el número de falsas alarmas por cada deslizamiento de tierra correctamente predecido sigue siendo alto. En este artículo, se reconoce la contribución de las alteraciones antropogénicas a los deslizamientos de tierra como uno de los principales obstáculos.

En el **Artículo III**, se propone un nuevo método para establecer umbrales de lluvia basado en la valoracón gráfica de la frecuencia de los eventos lluviosos. En este caso, se analizaron gráficos de lluvia detonante vs. lluvia antecedente para uno, dos, tres y cuatro días previos a la ocurrencia de deslizamientos de tierra. Se construyeron líneas de contorno para la frecuencia de lluvia en cada gráfico para mostrar cómo la frecuencia de los eventos lluviosos varía a medida que éstos se alejan del origen del gráfico. Este método tiene dos propósitos fundamentales. Primero, el número de falsas alarmas por cada deslizamiento de tierra correctamente predecido se redujo en un 20% con respecto al umbral propuesto en el **Artículo II**. Segundo, el umbral de doble límite permite identificar aquellos deslizamientos de tierra inducidos naturalmente por lluvia y los deslizamientos de tierra que requieren de fuerzas mayores de desestabilización del ser humano para predisponer las laderas hasta el punto en que eventos lluviosos ordinarios puedan ocasionar fallas.

El análisis espacial de los deslizamientos de tierra es abordado en el **Artículo IV**. Los tres factores preparatorios analizados fueron: la pendiente, la geología y la distancia a los ríos. Dos mapas de susceptibilidad fueron elaborados basados en el método matricial: el primero derivado del mapa de colonias afectadas por deslizamientos de tierra, que fue construido a partir de la base de datos de 26 años, y el segundo derivado de una interpretación de fotografías aéreas llevada a cabo en el 2014 por la Agencia Japonesa de Cooperación Internacional (JICA). La comparación de estos dos mapas de

susceptibilidad reveló que el mapa basado en la interpretación de fotografías aéreas proporciona mejores resultados en la identificación de los polígonos de los deslizamientos de tierra generados en el 2014 que el mapa basado en los archivos de prensa. También se ha demostrado que el bajo rendimiento del mapa basado en archivos de prensa se debe en parte al estado incompleto del inventario disponible en la base de datos, puesto que éste se ve afectado por la escasez de cobertura de los reportajes informativos en aréas no habitadas. En general, el mapa basado en archivos de prensa provee una sobreestimación de la vulnerabilidad a los deslizamientos de tierra de la ciudad.

Finalmente, en la discusión de la tesis se brinda una perspectiva de las ventajas y desventajas de la utilización de archivos de prensa en los estudios de deslizamientos de tierra. Los retos de analizar deslizamientos de tierra urbanos también han sido abordados. Además, se sugieren posibles usos de los estudios presentados en esta tesis para la preparación de Tegucigalpa para futuros deslizamientos de tierra.

12. References

Aguilar, E., Peterson, T. C., Obando, P. R., Frutos, R., Retana, J. A., Solera, M., . . . Mayorga, R. (2005). Changes in precipitation and temperature extremes in Central America and northern South America, 1961–2003. *J Geophys Res, 110*(D23), 1-15. doi:10.1029/2005JD006119

Akgun, A., Dag, S., & Bulut, F. (2008). Landslide susceptibility mapping for a landslide-prone area (Findikli, NE of Turkey) by likelihood-frequency ratio and weighted linear combination models. *Environ Geol, 54*(6), 1127-1143. doi:10.1007/s00254-007-0882-8

Alcántara-Ayala, I. (2008). On the historical account of disastrous landslides in Mexico: the challenge of risk management and disaster. *Adv Geosci, 14*, 159-164.

Alcántara-Ayala, I. (2002). Geomorphology, natural hazards, vulnerability and prevention of natural disasters in developing countries. *Geomorphology, 47*(2–4), 107-124. doi:10.1016/S0169-555X(02)00083-1

Alcántara-Ayala, I. (2009). Disasters in Mexico and Central America: A Little Bit More than a Century of Natural Hazards. In M. L. Edgardo (Ed.), *Dev Earth Surf Process* (Vol. 13, pp. 75-97): Elsevier.

Aleotti, P. (2004). A warning system for rainfall-induced shallow failures. *Eng Geol, 73*(3–4), 247-265. doi:10.1016/j.enggeo.2004.01.007

Alexander, D. (2005). Vulnerability to Landslides. In T. Glade, M. Anderson, & M. J. Crozier (Eds.), *Landslide Hazard and Risk* (pp. 175-198): John Wiley & Sons Ltd.

Alfaro, E. J. (2002). Some characteristics of the annual precipitation cycle in Central America and their relationship with its surrounding tropical oceans. *Top. Meteoro. Oceanog., 9*(2), 88-103.

Althuwaynee, O. F., Pradhan, B., & Ahmad, N. (2014). Estimation of rainfall threshold and its use in landslide hazard mapping of Kuala Lumpur metropolitan and surrounding areas. *Landslides*. doi:10.1007/s10346-014-0512-y

Angel, S., Bartley, K., & Derr, M. (2004). *Rapid Urbanization in Tegucigalpa, Honduras: Preparing for the Doubling of the City's Population in the Next Twenty-Five Years*.

Antronico, L., Borrelli, L., Coscarelli, R., Pasqua, A. A., Petrucci, O., & Gullà , G. (2013). Slope movements induced by rainfalls damaging an urban area: the Catanzaro case study (Calabria, southern Italy). *Landslides, 10*(6), 801-814. doi:10.1007/s10346-013-0431-3

Ayalew, L., & Yamagishi, H. (2005). The application of GIS-based logistic regression for landslide susceptibility mapping in the Kakuda-Yahiko Mountains, Central Japan. *Geomorphology, 65*(1–2), 15-31. doi:10.1016/j.geomorph.2004.06.010

Ayalew, L., Yamagishi, H., Marui, H., & Kanno, T. (2005). Landslides in Sado Island of Japan: Part II. GIS-based susceptibility mapping with comparisons of results from two methods and verifications. *Engineering Geology, 81*(4), 432-445. doi:10.1016/j.enggeo.2005.08.004

Ayalew, L., Yamagishi, H., & Ugawa, N. (2004). Landslide susceptibility mapping using GIS-based weighted linear combinations, the case in Tsugawa are of Agano River, Niigata Prefecture, Japan. *Landslides, 1*(1), 73-81. doi:10.1007/s10346-003-0006-9

Bai, S., Wang, J., Thiebes, B., Cheng, C., & Yang, Y. (2014). Analysis of the relationship of landslide occurrence with rainfall: a case study of Wudy County, China. *Arab J Geosci, 7*(4), 1277-1285. doi:10.1007/s12517-013-0939-9

Bommer, J. J., & Rodríguez, C. E. (2002). Earthquake-induced landslides in Central America. *Eng Geol, 63*(3–4), 189-220. doi:10.1016/S0013-7952(01)00081-3

Bui, D. T., Pradhan, B., Lofman, O., Revhaug, I., & Dick, Ã. y. B. (2013). Regional prediction of landslide hazard using probability analysis of intense rainfall in the Hoa Binh province, Vietnam. *Nat Hazards, 66*(2), 707-730. doi:10.1007/s11069-012-0510-0

Calcaterra, D., Parise, M., & Palma, B. (2003). Combining historical and geological data for the assessment of the landslide hazard: a case study from Campania, Italy. *Nat Hazards Earth Syst Sci, 3*, 3-16.

Calvello, M., d'Orsi, R. N., Piciullo, L., Paes, N., Magalhaes, M., & Lacerda, W. A. (2014). The Rio de Janeiro early warning system for rainfall-induced landslides: Analysis of performance for the years 2010–2013. *Int J Disaster Risk Reduct*(0). doi:10.1016/j.ijdrr.2014.10.005

Carrara, A., Crosta, G., & Frattini, P. (2003). Geomorphological and historical data in assessing landslide hazard. *Earth Surf Process Landforms, 28*(10), 1125-1142. doi:10.1002/esp.545

Cascini, L., Bonnard, C., Corominas, J., Jibson, R., & Montero-Olarte, J. (2005). Landslide hazard and risk zoning for urban planning and development. In O. Hungr, R. Fell, R. Couture, & E. Eberhardt (Eds.), *Landslide Risk Management* (pp. 199-235). London: Taylor and Francis.

Cepeda, J., Chavez, J. A., & Cruz Martinez, C. (2010). Procedure for the selection of runout model parameters from landslide back analyses: application to the Metropolitan Area of San Salvador, El Salvador. *Landslides, 7*(2), 105-116. doi:10.1007/s10346-010-0197-9

Cepeda, J., Höeg, K., & Nadim, F. (2010). Landslide-triggering rainfall thresholds: a conceptual framework. *Quarterly Journal of Engineering Geology and Hydrogeology, 43*(1), 69-84. doi:10.1144/1470-9236/08-066

Chatterjea, K. (2011). Severe wet spells and vulnerability of urban slopes: case of Singapore. *Nat Hazards, 56*(1), 1-18. doi:10.1007/s11069-009-9362-7

Chen, Z., & Wang, J. (2007). Landslide hazard mapping using logistic regression model in Mackenzie Valley, Canada. *Nat Hazards, 42*(1), 75-89. doi:10.1007/s11069-006-9061-6

Chleborad, A. F., Baum, R. L., & Godt, J. W. (2006). *Rainfall thresholds for forecasting landslides in the Seattle, Washington, Area - exceedance and probability*.

Chowdhury, R., & Flentje, P. (2002). Uncertainties in rainfall-induced landslide hazard. *Quarterly Journal of Engineering Geology and Hydrogeology, 35*(1), 61-69. doi:10.1144/qjegh.35.1.61

Clerici, A., Perego, S., Tellini, C., & Vescovi, P. (2002). A procedure for landslide susceptibility zonation by the conditional analysis method. *Geomorphology, 48*(4), 349-364. doi:10.1016/S0169-555X(02)00079-X

Costanzo, D., Rotigliano, E., Irigaray, C., Jiménez-Perálvarez, J., & Chacón, J. (2012). Factors selection in landslide susceptibility modelling on large scale following the gis matrix method: application to the river Beiro basin (Spain). *Nat. Hazards Earth Syst. Sci., 12*(2), 327-340. doi:10.5194/nhess-12-327-2012

Cross, M. (1998). Landslide susceptibility mapping using the matrix assessment approach: a Derbyshire case study. In J. Maund & M. Eddleston (Eds.), *Geohazards in Engineering Geology* (Vol. 15, pp. 247-261). London, UK: The Geological Society.

Cruden, D. M., & Varnes, D. J. (1996). Landslide types and processes. *Landslides-Investigation and Mitigation, Special Report, 247*, 36-75.

Dahal, R. K., & Hasegawa, S. (2008). Representative rainfall thresholds for landslides in the Nepal Himalaya. *Geomorphology, 100*(3–4), 429-443. doi:10.1016/j.geomorph.2008.01.014

Dahal, R. K., Hasegawa, S., Nonomura, A., Yamanaka, M., Dhakal, S., & Paudyal, P. (2008). Predictive modelling of rainfall-induced landslide hazard in the Lesser Himalaya of Nepal based on weights-of-evidence. *Geomorphology, 102*(3–4), 496-510. doi:10.1016/j.geomorph.2008.05.041

Dai, F., Lee, C., Tham, L., Ng, K., & Shum, W. (2004). Logistic regression modelling of storm-induced shallow landsliding in time and space on natural terrain of Lantau Island, Hong Kong. *Bull Eng Geol Environ, 63*(4), 315-327. doi:10.1007/s10064-004-0245-6

De Graff, J., Romesburg, H., Ahmad, R., & McCalpin, J. (2012). Producing landslide susceptibility maps for regional planning in data scarce regions. *Nat Hazards, 64*(1), 729-749. doi:10.1007/s11069-012-0267-5

de Souza, F., & Ebecken, N. (2012). A data based model to predict landslides induced by rainfall in Rio de Janeiro City. *Geotech Geol Eng, 30*(1), 85-94. doi:10.1007/s10706-011-9451-8

DESINVENTAR. (2013). Red de estudios sociales en prevencion de desastres naturales en America Latina. Retrieved 5 of February, 2013 http://online.desinventar.org/desinventar/#HND-20101004

Devoli, G., Morales, A., & Hoeg, K. (2007a). Historical Landslides in Nicaragua - Collection and Analysis of Data. *Landslides, 4*, 5-18. doi:10.1007/s10346-006-0048-x

Devoli, G., Strauch, W., Chavez, G., & Hoeg, K. (2007b). A Landslide Database for Nicaragua: A Tool for Landslide-Hazard Management. *Landslides, 4*(2), 163-176. doi:10.1007/s10346-006-0074-8

Domínguez Cuesta, M. a. J., Jiménez Sánchez, M., & Rodríguez García, A. (1999). Press archives as temporal records of landslides in the North of Spain: relationships between rainfall and instability slope events. *Geomorphology, 30*(1–2), 125-132. doi:10.1016/S0169-555X(99)00049-5

Duman, T. Y., Can, T., Gokceoglu, C., Nefeslioglu, H. A., & Sonmez, H. (2006). Application of logistic regression for landslide susceptibility zoning of Cekmece Area, Istanbul, Turkey. *Environ Geol, 51*(2), 241-256. doi:10.1007/s00254-006-0322-1

ECLAC. (1999). *Honduras: Assessment of the Damage Caused by Hurricane Mitch, 1998. Implications for Economic and Social Development and for the Environment.* Retrieved from Mexico: http://www.eclac.org/cgi-bin/getProd.asp?xml=/publicaciones/xml/6/15506/P15506.xml&xsl=/mexico/tpl-i/p9f.xsl&base=/mexico/tpl/top-bottom.xsl

El Heraldo. (2013). Al menos seis invasiones surgen al ano en la capital de Honduras. *El Heraldo*. Retrieved from http://www.elheraldo.hn/Secciones-Principales/Metro/Al-menos-seis-invasiones-al-ano-surgen-en-la-capital-de-Honduras#panel1-2

El Heraldo. (2014). Identifican 1,500 áreas de deslizamiento en la capital. *El Heraldo*. Retrieved from http://www.elheraldo.hn/csp/mediapool/sites/ElHeraldo/Metro/story.csp?cid=588018&sid=298&fid=213

El Heraldo. (2015). Crean plan de vivienda para arrendatarios. *El Heraldo*. Retrieved from http://www.elheraldo.hn/metro/870766-213/crean-plan-de-vivienda-para-arrendatarios

Erener, A., & Duzgun, H. B. S. (2013). A regional scale quantitative risk assessment for landslides: a case of Kumluca watershed in Bartin, Turkey. *Landslides, 10*(1), 55-73. doi:10.1007/s10346-012-0317-9

Fay, M., Ghesquiere, F., & Solo, T. (2003) Desastres Naturales y Pobres Urbanos. *En Breve* (32 ed.): World Bank.

Fernández, T., Irigaray, C., El Hamdouni, R., & Chacón, J. (2003). Methodology for landslide susceptibility mapping by means of a GIS. Application to the Contraviesa area (Granada, Spain). *Nat. Hazards, 30*(3), 297-308. doi:10.1023/B:NHAZ.0000007092.51910.3f

Flores Peñalba, R., Luo, Z., & Juang, C. H. (2009). Framework for probabilistic assessment of landslide: a case study of El Berrinche. *Environ Earth Sci, 59*(3), 489-499. doi:10.1007/s12665-009-0046-0

Floris, M., & Bozzano, F. (2008). Evaluation of landslide reactivation: a modified rainfall threshold model based on historical records of rainfall and landslides. *Geomorphology, 94*(1), 40-57. doi:10.1016/j.geomorph.2007.04.009

Foster, C., Pennington, C. V. L., Culshaw, M. G., & Lawrie, K. (2012). The national landslide database of Great Britain: development, evolution and applications. *Environ Earth Sci, 66*(3), 941-953. doi:10.1007/s12665-011-1304-5

Frattini, P., Crosta, G., & Sosio, R. (2009). Approaches for defining thresholds and return periods for rainfall-triggered shallow landslides. *Hydrol. Process., 23*(10), 1444-1460. doi:10.1002/hyp.7269

Frigerio, S., & van Westen, C. (2010). RiskCity and WebRiskCity: Data Collection, Display, and Dissemination in a Multi-Risk Training Package. *Cartography Geog Inf Sci, 37*(2), 119-135. doi:10.1559/152304010791232190

Gabet, E. J., Burbank, D. W., Putkonen, J. K., Pratt-Sitaula, B. A., & Ojha, T. (2004). Rainfall thresholds for landsliding in the Himalayas of Nepal. *Geomorphology, 63*(3–4), 131-143. doi:10.1016/j.geomorph.2004.03.011

Glade, T. (2001). Landslide Hazard Assessment and Historical Landslide Data - An Inseparable Couple? *The use of historical data in natural hazar assessments* (pp. 153-168). Netherlands: Kluwer Academic Publishers.

Guzzetti, F. (2000). Landslide fatalities and the evaluation of landslide risk in Italy. *Eng Geol, 58*(2), 89-107. doi:10.1016/S0013-7952(00)00047-8

Guzzetti, F., Peruccacci, S., Rossi, M., & Stark, C. P. (2007). Rainfall thresholds for the initiation of landslides in central and southern Europe. *Meteorol Atmos Phys, 98*(3-4), 239-267. doi:10.1007/s00703-007-0262-7

Guzzetti, F., Stark, C., & Salvati, P. (2005). Evaluation of Flood and Landslide Risk to the Population of Italy. *Environ Manag, 36*(1), 15-36. doi:10.1007/s00267-003-0257-1

Harp, E. L., Castañeda, M., & Held, M. D. (2002). Landslides triggered by Hurricane Mitch in Tegucigalpa, Honduras: U.S. Geologic Survey Open File Report 02-0033.

Harp, E. L., Reid, M. E., McKenna, J. P., & Michael, J. A. (2009). Mapping of hazard from rainfall-triggered landslides in developing countries: Examples from Honduras and Micronesia. *Eng Geol, 104*(3–4), 295-311. doi:10.1016/j.enggeo.2008.11.010

Hilker, N., Badoux, A., & Hegg, C. (2009). The Swiss flood and landslide damage database 1972-2007. *Nat Hazards Earth Syst Sci, 9*(3), 913-925.

Huggel, C., Khabarov, N., Obersteiner, M., & Ramírez, J. (2010). Implementation and integrated numerical modeling of a landslide early warning system: a pilot study in Colombia. *Nat Hazards, 52*(2), 501-518. doi:10.1007/s11069-009-9393-0

Ibsen, M.-L., & Brunsden, D. (1996). The nature, use and problems of historical archives for the temporal occurrence of landslides, with specific reference to the south coast of Britain, Ventnor, Isle of Wight. *Geomorphology, 15*(3–4), 241-258. doi:10.1016/0169-555X(95)00073-E

Ibsen, M.-L., & Casagli, N. (2004). Rainfall patterns and related landslide incidence in the Porretta-Vergato region, Italy. *Landslides, 1*(2), 143-150. doi:10.1007/s10346-004-0018-0

Irigaray, C., Fernández, T., El Hamdouni, R., & Chacón, J. (2007). Evaluation and validation of landslide susceptibility maps obtained by a GIS matrix method: examples from the Betic Cordillera (southern Spain). *Nat. Hazards, 41*(1), 61-79. doi:10.1007/s11069-006-9027-8

Jaiswal, P., & van Westen, C. J. (2009). Estimating temporal probability for landslide initiation along transportation routes based on rainfall thresholds. *Geomorphology, 112*(1–2), 96-105. doi:10.1016/j.geomorph.2009.05.008

Jemec, M., & Komac, M. (2012). Rainfall patterns for shallow landsliding in perialpine Slovenia. *Nat Hazards, 67*(3), 1011-1023. doi:10.1007/s11069-011-9882-9

JICA. (2002). *The Study on Flood Control and Landslide Prevention in Tegucigalpa Metropolitan Area of the Republic of Honduras*. Retrieved from Tegucigalpa, Honduras:

Jiménez-Perálvarez, J. D., Irigaray, C., El Hamdouni, R., & Chacón, J. (2009). Building models for automatic landslide susceptibility analysis, mapping and validation in ArcGIS. *Nat Hazards, 50*(3), 571-590. doi:10.1007/s11069-008-9305-8

Jiménez-Perálvarez, J. D., Irigaray, C., El Hamdouni, R., & Chacón, J. (2011). Landslide-susceptibility mapping in a semi-arid mountain environment: an example from the southern slopes of Sierra Nevada (Granada, Spain). *Bull Eng Geol Environ, 2011*(2), 265-277. doi:10.1007/s10064-010-0332-9

Kalantzi, F., Doutsou, I., & Koukouvelas, I. (2010). Historical Landslides in the Prefecture of Ioannina - Collection and Analysis of Data. *Bull Geol Soc Greece, 43*(3), 1350-1360.

Kanungo, D. P., & Sharma, S. (2014). Rainfall thresholds for prediction of shallow landslides around Chamoli-Joshimath region, Garhwal Himalayas, India. *Landslides, 11*(4), 629-638. doi:10.1007/s10346-013-0438-9

Khan, Y. A., Lateh, H., Baten, M. A., & Kamil, A. A. (2012). Critical antecedent rainfall conditions for shallow landslides in Chittagong City of Bangladesh. *Environ Earth Sci, 67*(1), 97-106. doi:10.1007/s12665-011-1483-0

Kirschbaum, D., Adler, R., Adler, D., Peters-Lidard, C., & Huffman, G. (2012). Global Distribution of Extreme Precipitation and High-Impact Landslides in 2010 Relative to Previous Years. *Journal of Hydrometeorology, 13*(5), 1536-1551. doi:10.1175/JHM-D-12-02.1

Kirschbaum, D., Stanley, T., & Simmons, J. (2015a). A dynamic landslide hazard assessment system for Central America and Hispaniola. *Nat Hazards Earth Sys Sci Discuss, 3*, 2847-2882. doi:10.5194/nhessd-3-2847-2015

Kirschbaum, D., Stanley, T., & Yatheendradas, S. (2015b). Modeling landslide susceptibility over large regions with fuzzy overlay. *2015*. doi:10.1007/s10346-015-0577-2

Kirschbaum, D. B., Adler, R., Hong, Y., Hill, S., & Lerner-Lam, A. (2010). A Global Landslide Catalog for Hazard Applications: Method, Results and Limitations. *Nat Hazards, 52*, 561-575. doi:10.1007/s11069-009-9401-4

Klimes, J., & Rios Escobar, V. (2010). A landslide susceptibility assessment in urban areas based on existing data: an example from the Iguaná Valley, Medellín City, Colombia. *Nat. Hazards Earth Syst. Sci., 10*(10), 2067-2079. doi:10.5194/nhess-10-2067-2010

Kreft, S. E., D.Junghans, L.Kerestan, C.Hagen, U. (2014). *Global Climate Risk Index 2015*. Retrieved from http://germanwatch.org/en/9470

Larsen, M. C. (2008). Rainfall-triggered landslides, anthropogenic hazards, and mitigation strategies. *Adv Geosci, 14*, 147-153. doi:10.5194/adgeo-14-147-2008

Lee, S., & Pradhan, B. (2007). Landslide hazard mapping at Selangor, Malaysia using frequency ratio and logistic regression models. *Landslides, 4*(1), 33 - 41. doi:10.1007/s10346-006-0047-y

Lee, S., & Sambath, T. (2006). Landslide susceptibility mapping in the Damrei Romel area, Cambodia using frequency ratio and logistic regression models. *Environ. Geol, 50*(6), 847-855. doi:10.1007/s00254-006-0256-7

Lepore, C., Kamal, S. A., Shanahan, P., & Bras, R. L. (2012). Rainfall-induced landslide susceptibility zonation of Puerto Rico. *Environ Earth Sci, 66*(6), 1667 - 1681. doi:10.1007/s12665-011-0976-1

Li, C., Ma, T., Zhu, X., & Li, W. (2011). The power–law relationship between landslide occurrence and rainfall level. *Geomorphology, 130*(3–4), 221-229. doi:10.1016/j.geomorph.2011.03.018

Llasat, M., Llasat-Botija, M., & Lopez, L. (2009). A press database on natural risks and its applications in the study of floods in Northeastern Spain. *Nat Hazards Earth Syst Sci, 9*, 2049-2061.

Marchi, L., & Tecca, P. (2006). Some Observations on the Use of Data from Historical Documents in Debris-Flow Studies. *Nat Hazards, 38*(3), 301-320. doi:10.1007/s11069-005-0264-z

Marques, R., Zêzere, J., Trigo, R., Gaspar, J., & Trigo, I. (2008). Rainfall patterns and critical values associated with landslides in Povoação County (São Miguel Island, Azores): relationships with the North Atlantic Oscillation. *Hydrol Process, 22*(4), 478-494. doi:10.1002/hyp.6879

Mathew, J., Babu, D. G., Kundu, S., Kumar, K. V., & Pant, C. C. (2013). Integrating intensity-duration-based rainfall threshold and antecedent rainfall-based probability estimate towards generating early warning for rainfall-induced landslides in parts of the Garhwal Himalaya, India. *Landslides*, 1-14. doi:10.1007/s10346-013-0408-2

Melchiorre, C., Matteucci, M., Azzoni, A., & Zanchi, A. (2008). Artificial neural networks and cluster analysis in landslide susceptibility zonation. *Geomorphology, 94*(3–4), 379-400. doi:10.1016/j.geomorph.2006.10.035

Mora, S. (2009). Disasters are not natural: risk management, a tool for development. In M. G. Culshaw, H. J. Reeves, I. Jefferson, & T. W. Spink (Eds.), *Engineering Geology for Tomorrow's Cities* (Engineering Geology Special Publications ed., Vol. 22, pp. 101 - 112). London: The Geological Society.

Nadim, F., Cepeda, J., Sandersen, F., Jaedicke, C., & Heyerdahl, H. (2009). *Prediction of rainfall-induced landslides through empirical and numerical models*. Paper presented at the First Italian Workshop on Landslides, Rainfall-induced landslides: mechanisms, monitoring techniques and nowcasting models for early-warning systems, Naples, Italy.

Nadim, F., Kjekstad, O., Peduzzi, P., Herold, C., & Jaedicke, C. (2006). Global landslide and avalanche hotspots. *Landslides, 3*(2), 159-173. doi:10.1007/s10346-006-0036-1

Pardeshi, S. D., Autade, S. E., & Pardeshi, S. S. (2013). Landslide hazard assessment: recent trends and techniques. *SpringerPlus, 2*(1), 523. doi:10.1186/2193-1801-2-523

Pearce-Oroz, G. (2005). Causes and consequences of rapid urban spatial segregation. In D. Varady (Ed.), *Desegragating The City: Ghettos, Enclaves and Inequality* (pp. 108-124): Suny Press.

Petley, D. N. (2009). On the impact of urban landslides. In M. G. Culshaw, H. J. Reeves, I. Jefferson, & T. W. Spink (Eds.), *Engineering Geology for Tomorrow´s Cities* (Vol. 22, pp. 83-99). London: Geological Society.

Petley, D. N., Dunning, S. A., & Rosser, N. J. (2005). The Analysis of Global Landslide Risk Through the Creation of a Database of Worldwide Landslide Fatalities. In O. Hungr, R. Fell, R. Counture, & E. Ebergardt (Eds.), *Landslide Risk Management* (pp. 367-374). Balkema, Amsterdam.

Petrucci, O., & Pasqua, A. (2009). A methodological approach to characterise Landslide Periods based on historical series of rainfall and landslide damage. *Nat Hazards Earth Syst Sci, 9*(5), 1655-1670. doi:10.5194/nhess-9-1655-2009

Petrucci, O., & Polemio, M. (2003). The use of historical data for the characterisation of multiple damaging hydrogeological events. *Nat Hazards Earth Syst Sci, 3*, 17-30.

Petrucci, O., Polemio, M., & Pasqua, A. A. (2009). Analysis of Damaging Hydrogeological Events: The Case of the Calabria Region (Southern Italy). *Environ Manag, 43*(3), 483-495. doi:10.1007/s00267-008-9234-z

Pielke, R. A., Rubiera, J., Landsea, C., Fernandez, M. L., & Klein, R. (2003). Hurricane Vulnerability in Latin America and the Caribbean: Normalized Damage and Loss Potentials. *Nat Hazards Rev, 4*(3), 101-114. doi:10.1061/(ASCE)1527-6988(2003)4:3(101)

Pineda, M. A. (2004). *Identificación y análisis de las áreas susceptibles de los procesos de remoción en masa, en la cuenca alta del rio Grande o Choluteca, en Tegucigalpa, Honduras.C.A.* (Masters Degree Thesis), Universidad de Costa Rica.

Polemio, M., & Sdao, F. (1999). The role of rainfall in the landslide hazard: the case of the Avigliano urban area (Southern Apennines, Italy). *Engineering Geology, 53*(3–4), 297-309. doi:10.1016/S0013-7952(98)00083-0

Pradhan, B., & Lee, S. (2010). Delineation of landslide hazard areas on Penang Island, Malaysia, by using frequency ratio, logistic regression, and artificial neural network models. *Environ Earth Sci, 60*(5), 1037 - 1054. doi:10.1007/s12665-009-0245-8

Raska, P., Klimes, J., & Dubisar, J. (2013). Using local archive sources to reconstruct historical landslide occurrence in selected urban regions of the Czech Republic: examples from regions with different historical development. *Land Degrad Develop*, 1099-1145x. doi:10.1002/ldr.2192

Regmi, N. R., Giardino, J. R., & Vitek, J. D. (2010). Modeling susceptibility to landslides using the weight of evidence approach: Western Colorado, USA. *Geomorphology, 115*(1–2), 172-187. doi:10.1016/j.geomorph.2009.10.002

Schuster, R., & Highland, L. (2007). The Third Hans Cloos Lecture. Urban landslides: socioeconomic impacts and overview of mitigative strategies. *Bulletin of Engineering Geology and the Environment, 66*(1), 1-27. doi:10.1007/s10064-006-0080-z

Sengupta, A., Gupta, S., & Anbarasu, K. (2010). Rainfall thresholds for the initiation of landslide at Lanta Khola in north Sikkim, India. *Nat Hazards, 52*(1), 31-42. doi:10.1007/s11069-009-9352-9

Sepúlveda, S. A., & Petley, D. N. (2015). Regional trends and controlling factors of fatal landslides in Latin America and the Caribbean. *Nat. Hazards Earth Syst. Sci., 3*, 1821-1833. doi:10.5194/nhess-15-1821-2015

Süzen, M. L., & Doyuran, V. (2004). A comparison of the GIS based landslide susceptibility assessment methods: multivariate versus bivariate. *Environ. Geolog., 45*(5), 665-679. doi:10.1007/s00254-003-0917-8

Terlien, M. T. (1998). The determination of statistical and deterministic hydrological landslide-triggering thresholds. *Environ Geol, 35*(2-3), 124-130. doi:10.1007/s002540050299

Tropeano, D., & Turconi, L. (2004). Using Historical Documents for Landslide, Debris Flow and Stream Flood Prevention. Applications in Northern Italy. *Nat Hazards, 31*, 663-679. doi:10.1023/B:NHAZ.0000024897.71471.f2

UNDP-DIPECHO. (2010). *14 Barrios Vulnerables a Deslizamientos y Sismos en la Ciudad*. Retrieved from http://riesgosydesarrollo.org/?cat=1103&title=Proyecto%20DIPECHO%20VII(=es

UNDP-DIPECHO. (2012). *Reduciendo riesgos por deslizamientos y sismos en Tegucigalpa, 2010-2012: 15 barrios vulnerables a deslizamientos y sismos en la ciudad de Tegucigalpa*. Retrieved from http://riesgosydesarrollo.org/web/odm_data/rt/Estudio%20comparativo%20de%20la%20l%C3%83%C2%ADnea%20base%20del%20proyecto%20en%2015%20barrios%20vulnerables%20de%20Tegucigalpa,%20PNUDGOAL.%202012.%20(PDF).pdf

UN-Habitat. (2012). Towards a new urban transition *The State of Latin American and Caribbean Cities* (2012 ed., pp. 194): United Nations Human Settlement Programme.

Vakis, R. R., J.Lucchetti, L. (2015). Left behind: Chronic poverty in Latin American and the Caribbean.

van Westen, C. J., Castellanos, E., & Kuriakose, S. L. (2008). Spatial data for landslide susceptibility, hazard, and vulnerability assessment: An overview. *Eng Geol, 102*(3–4), 112-131. doi:10.1016/j.enggeo.2008.03.010

Vranken, L., Vantilt, G., Van Den Eeckhaut, M., Vandekerckhove, L., & Poesen, J. (2015). Landslide risk assessment in a densely populated hilly area. *Landslides, 12*(4), 787-798. doi:10.1007/s10346-014-0506-9

Westerberg, I., Walther, A., Guerrero, J. L., Coello, Z., Halldin, S., Xu, C. Y., . . . Lundin, L. C. (2010). Precipitation data in a mountainous catchment in Honduras: quality assessment and spatiotemporal characteristics. *Theor Appl Climatol, 101*(3-4), 381-396. doi:10.1007/s00704-009-0222-x

Winter, M. G., & Bromhead, E. N. (2012). Landslide risk: some issues that determine societal acceptance. *Nat Hazards, 62*(2), 169-187. doi:10.1007/s11069-011-9987-1

Yalcin, A., Reis, S., Aydinoglu, A. C., & Yomralioglu, T. (2011). A GIS-based comparative study of frequency ratio, analytical hierarchy process, bivariate statistics and logistics regression methods for landslide susceptibility mapping in Trabzon, NE Turkey. *CATENA, 85*(3), 274-287. doi:10.1016/j.catena.2011.01.014

Yamagishi, H., Yagi, H., & Sato, G. (2014). *Landslide hazard mapping of Tegucigalpa, Honduras - capacity building by JICA-JSPS Project (2012 to 2014).* Paper presented at the Proceedings of World Landslide Forum 3, 2-6 June 2014, Bejing, China.

Zezêre, J. L., Vaz, T., Pereira, S., Oliveira, S. C., Marques, R., & Garcia, R. A. C. (2015). Rainfall thresholds for landslide activity in Portugal: a state of the art. *Environ Earth Sci, 73*(6), 2917-2936. doi:10.1007/s12665-014-3672-0

Zêzere, J. L., Reis, E., Garcia, R., Oliveira, S., Rodrigues, M. L., Vieira, G., & Ferreira, A. B. (2004). Integration of spatial and temporal data for the definition of different landslide hazard scenarios in the area north of Lisbon (Portugal). *Nat. Hazards Earth Syst. Sci., 4*, 133-146.

Acta Universitatis Upsaliensis

Digital Comprehensive Summaries of Uppsala Dissertations from the Faculty of Science and Technology 1304

Editor: The Dean of the Faculty of Science and Technology

A doctoral dissertation from the Faculty of Science and Technology, Uppsala University, is usually a summary of a number of papers. A few copies of the complete dissertation are kept at major Swedish research libraries, while the summary alone is distributed internationally through the series Digital Comprehensive Summaries of Uppsala Dissertations from the Faculty of Science and Technology. (Prior to January, 2005, the series was published under the title "Comprehensive Summaries of Uppsala Dissertations from the Faculty of Science and Technology".)

Distribution: publications.uu.se
urn:nbn:se:uu:diva-264645

ACTA
UNIVERSITATIS
UPSALIENSIS
UPPSALA
2015